Thermo-Calc Software

TCS Mg-based Alloys Database (TCMG)

Validation and Calculation Examples Collection

Document created 2025-05-28

Contents

About the Database Examples

The *Validation and Calculation Examples Collection* that is available for many databases demonstrates both the *validity* of the database itself as well as demonstrates some of its *calculation* capabilities when combined with Thermo-Calc software and its Add-on Modules and features.

For each database, the type and number of available examples varies. In some cases an example can belong to both a validation and calculation type.

- *Validation* examples generally include experimental data in the plot or diagram to show how close to the predicted data sets the Thermo-Calc calculations are. It uses the most recent version of the software and relevant database(s) unless otherwise specified.
- *Calculation* examples are intended to demonstrate a use case of the database. This might be showing a binary or ternary system calculated in a phase diagram, or demonstrate how the database and relevant software features would be applied to a heat treatment application, process metallurgy, soldering process, and so forth. In the case of heat treatment, it might include the result of calculating solidification segregation, determining homogenization temperature and then predicting the time needed to homogenize. There are many other examples specifically related to each database.

Where relevant, most references related to each example set are included at the end of the individual section. You can also find additional references specific to the database itself when using the database within Thermo-Calc. You can also contact us directly should you have any questions.

If you are interested in sharing your own examples using Thermo-Calc products in unique or surprising ways, or if you want to share your results from a peer reviewed paper, send an email to info@thermocalc.com.

TCS Mg-based Alloys Database (TCMG) Resources

Information about the database is available on our website and in the Thermo-Calc software online Help.

- **Website**: On our website the information is both searchable and the database specific PDFs are available to download.
- **Online Help**: Technical database information is included with the Thermo-Calc software online Help. When in Thermo-Calc, press F1 to search for the same information as is contained in the PDF documents described. Depending on the database, there are additional examples available on the website.

Database Specific Documentation

- The *TCS Mg-based Alloys Database (TCMG) Technical Information* PDF document contains version specific information such as the binary, ternary, and higher-order assessed systems, phases and models. It also includes details about the properties data (e.g. viscosity, surface tension, etc.), a list of the included elements, and summaries of the database revision history by version.
- The *TCS Mg-based Alloys Database (TCMG) Validation and Calculation Examples Collection* PDF document contains a series of validation examples using experimental data, and a set of calculation examples showing some of the ways the database can be used.

Go to the Magnesium-based Alloys Databases page on our website where you can access a Validation and Calculation Examples Collection and the Technical Information plus learn more about the compatible kinetic database. Also explore further applications of Thermo-Calc to magnesium including links to resources such as examples, publications, and more.

The CALPHAD Method

The Thermo-Calc databases are developed with the CALPHAD approach based on various types of experimental data and theoretical values (e.g. those from first-principles calculations). It is based on the critical evaluation of binary, ternary, and for some databases, important higher order systems. This enables predictions to be made for multicomponent systems and alloys of industrial importance. Among these, the thermodynamic database is of fundamental importance.

Learn more on our website about the CALPHAD Method and how it is applied to the Thermo-Calc databases. Also visit the video tutorials on our website or our YouTube playlist.

TCMG Validation Examples

Some diagrams are calculated with earlier versions of the database. Negligible differences might be observed if these are recalculated with the most recent version. The diagrams are updated when there are considerable or significant improvements.

In this section:

Vertical Sections

Thermodynamic descriptions of core binary, ternary, and quaternary systems are of fundamental importance to the TCS Mg-based Alloys Database (TCMG). Such descriptions are derived from thermodynamic modeling based on phase equilibria data and thermodynamic properties. Once available, these can be used for predicting phase equilibria in the validated composition and temperature space.

Typical phase diagrams are isothermal sections and vertical sections. In these examples, typical vertical sections of several core ternary systems and the Mg-Al-Mn-Zn quaternary system are shown. Such diagrams can be of practical applications as well, e.g. making a preliminary determination of the heating temperature for melting, solution treatment, homogenization, and aging for specific alloys.

Ag-Mg-Sn

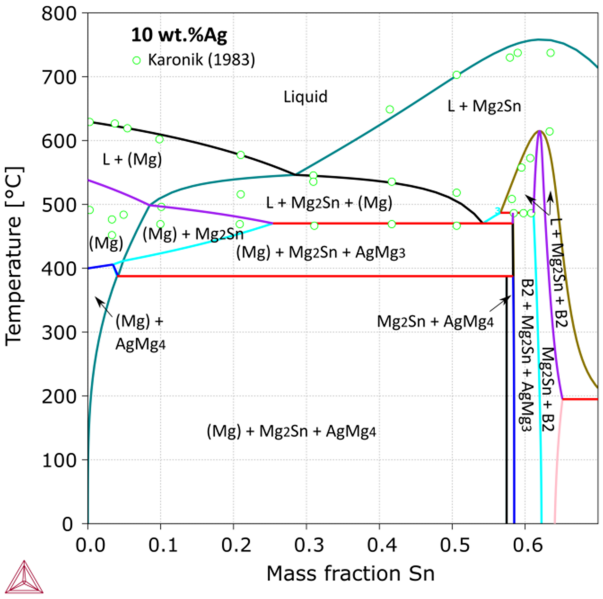

Figure 1: Calculated Ag-Mg-Sn vertical section at 10 wt.% Ag [2018Che], compared with experimental data [1983Kar].

Al-Mg-Sn

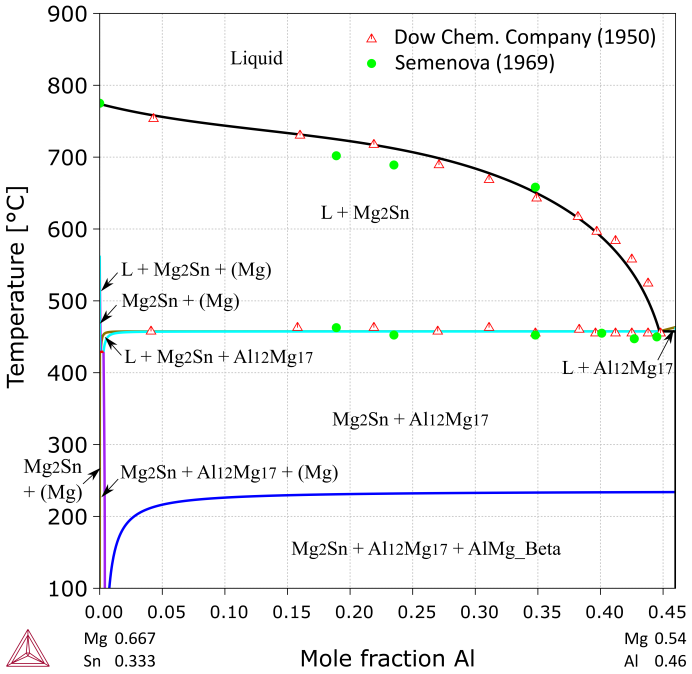

Figure 2: Calculated vertical section from $Mg_{0.667}Sn_{0.333}$ to $Mg_{0.54}Al_{0.46}$ (at.%) Experimental data cited in [2007Doe].

Ce-Mg-Mn

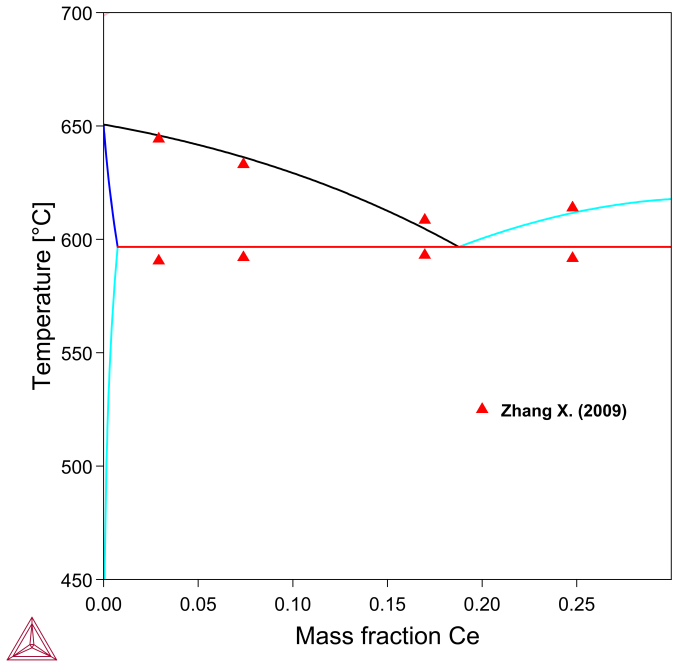

Figure 3: Calculated Ce-Mg-Mn vertical section at 2.5 wt. % Mn, compared with experimental data from [2009Zha].

Mg_2Sn-Mg_2Zn

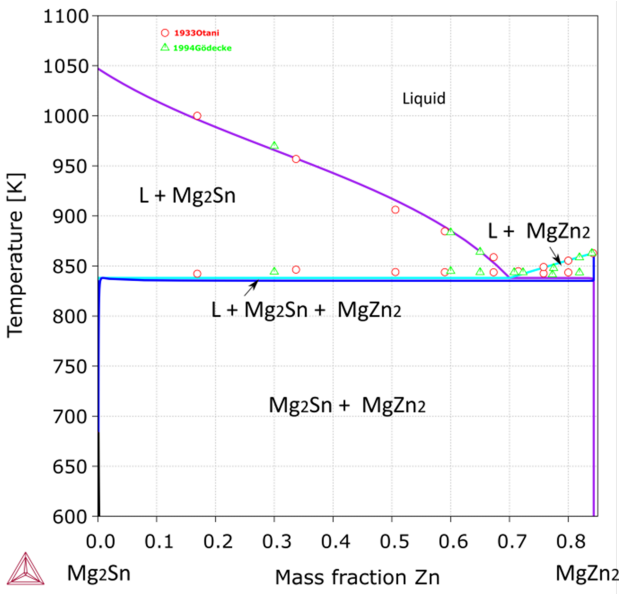

Figure 4: Calculated vertical section from Mg_2Sn to $MgZn_2$ [2010Men], compared with experimental data [1933Ota].

Mg-Al-Mn-Zn

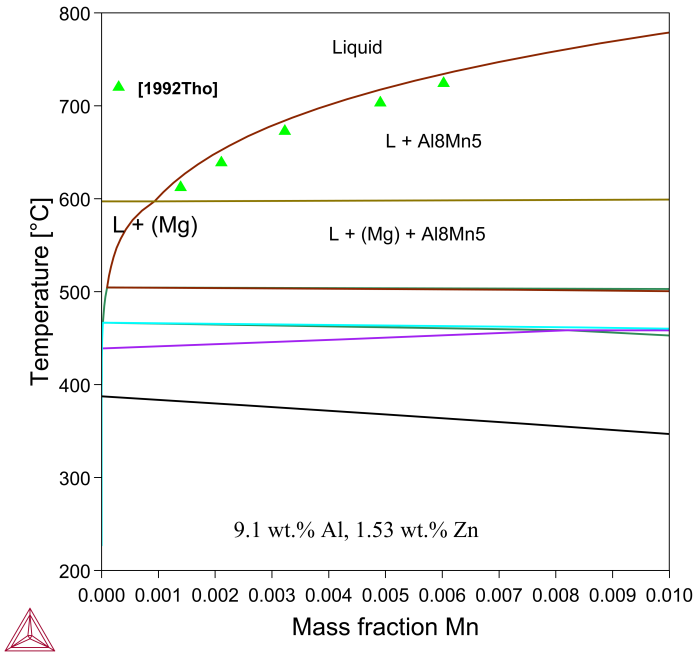

Figure 5: Calculated vertical section at 9.1 wt.% Al -1.53 wt.% Zn with Mn varying from 0 to 1 wt.% in the Mg-Al-Mn-Zn system. The experimental data are from [1992Tho].

References

[1933Ota] B. Otani, Constitution of the Phase Equilibrium Diagram of the Magnesium-Zinc-Tin System (in Japanese), Tetsu-to-Hagane, vol. 19, no. 7, pp. 566–574 (1933).

[1983Kar] V. V. Karonik, V. E. Kolesnichenko, A. A. Shepelev, and G. I. Kand, Magnesium-Silver-Tin Phase Diagram, Met. Splav. na Osn. Tsv. Met. M, no. 78–84 (1983).

[1992Tho] A. Thorvaldsen, C. A. Aliravci, Adv. Prod. Fabr. Light Met. Met. Matrix Comp., in Proceedings of the International Symposium, p. 277 (1992).

[2007Doe] E. Doernberg, A. Kozlov, R. Schmid-Fetzer, Experimental Investigation and Thermodynamic Calculation of Mg-Al-Sn Phase Equilibria and Solidification Microstructures. J. Phase Equilibria Diffus. 28, 523–535 (2007)

[2009Zha] X. Zhang, D. Kevorkov, I.-H. Jung, M. O. Pekguleryuz, Phase equilibria on the ternary Mg–Mn–Ce system at the Mg-rich corner. J. Alloys Compd. 482, 420–428 (2009).

[2010Men] F. G. Meng, J. Wang, L. B. Liu, and Z. P. Jin, Thermodynamic modeling of the Mg–Sn–Zn ternary system, J. Alloys Compd., vol. 508, no. 2, pp. 570–581 (2010).

[2018Che] H.-L. Chen, Thermodynamic assessment of the Ag-Mg-Sn system in TCMG5, Thermo-Calc Software (2018).

Mg-Y-Zn(-Zr) Alloys

Rare earth elements are major alloying elements or important additives in a wide range of Mg alloys. They help to improve high-temperature strength and creep resistance. The investigation of Mg-RE-TM alloys has attracted extra interest due to the finding of the long-period stacking-ordered (LPSO) phases.

RE = rare earth element, such as Gd, Tb, Dy, Ho, Er, Tm, or Y and TM = mostly transition metals such as Co, Ni, Cu, and Zn or the post-transition metal Al.

Also see another example about Long-period Stacking-ordered (LPSO) Structures.

The (0001) basal slip dominates the plastic deformation of the LPSO phase and the deformation kinks form when the basal slip is suppressed. The plastic anisotropy of the LPSO phase significantly contributes to the strengthening of (Mg)/LPSO two-phase alloys by enhancing grain refinement of the (Mg) grains. Among the Mg-RE-TM alloy systems, Mg-Y-Zn has been most extensively investigated and it forms the two most common types of LPSO structures, 14H and 18R.

The TCS Mg-based Alloys Database (TCMG) is used in this example to examine these Mg-Y-Zn(-Zr) alloys. Figure 6 shows the calculated Mg-Y-Zn liquidus projection in the Mg-rich region, which is validated with experimental results from as-cast Mg-Y-Zn(-Zr) alloys.

A small amount of Zr does not change the formation of major phases.

Phase formation sequences are marked for the most Mg-rich alloys in the range of < 10 at.% Y and < 25 at.% Zn. Not only the primary crystallization regions but also the compositions of the invariant equilibria agree with experimental data. As you can see, two arbitrary dividing lines “ab” and “cd” can be drawn based on the phase formation sequences and they extend towards “E 576” and “U 485”, respectively.

For the rest of the alloy compositions, at which only primary solidifying phases are known, the results can also be well accounted for. The 14H phase can only form via solid phase transformations. Its existence can be seen in the isothermal section at 773 K (Figure 7).

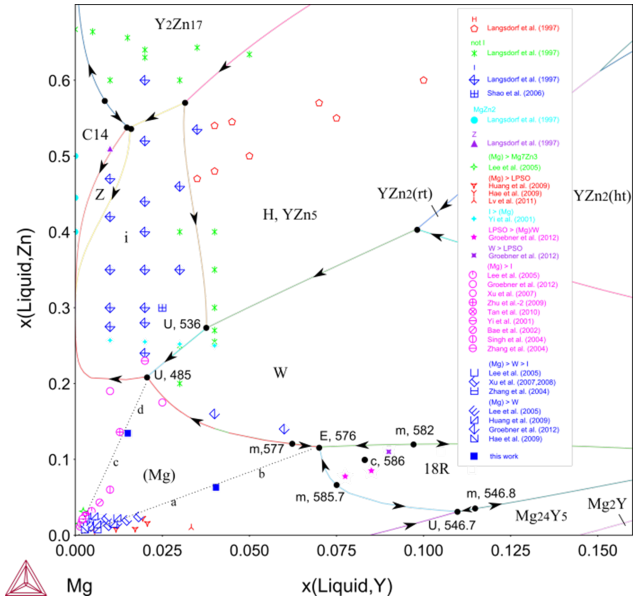

Figure 6: Calculated Mg-Y-Zn liquidus projection in the Mg-rich corner and the Mg-Zn vicinity [2015Che].

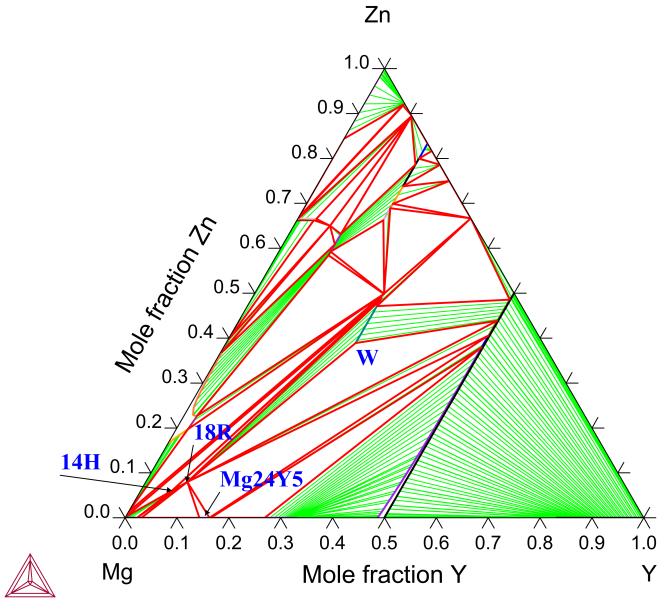

Figure 7: Calculated Mg-Y-Zn isothermal section at 773 K, showing the presence of 14H (LPSO), 18R (LPSO), W (Mg3R), I, Z, and H (YZn5) [2015Che].

Reference

[2015Che] H. Chen, Thermodynamic assessment of the Gd-Mg-Zn and Mg-Y-Zn systems in TCMG4, Thermo-Calc Software (2015).

Liquidus and Solidus Temperatures

The TCS Mg-based Alloys Database (TCMG) can be used to predict the liquidus and solidus temperatures, as well as incipient melting temperatures, which are critical to design heat treatments and melting processes.

This example plot compares calculated and measured liquidus temperatures and solidus temperatures, as well as incipient temperatures, from about 200 magnesium alloys. These are mostly customized alloys from the literature and include about 30 industrial alloys.

It should be noted that when such a temperature was determined with thermal analysis, the thermal effect must be large enough to be detected. Because of this, as-measured liquidus temperatures often do not accord with the start precipitation of the very first solid phase, if its amount is negligible. As-measured solidus temperatures could be before the alloys had fully solidified. In order to account for such uncertainties in experiments, the temperature at 99.5 % liquid is used as calculated liquidus temperature and that at 0.5% liquid as calculated solidus temperature. Calculated incipient temperatures are taken from Scheil simulations (at 0.5 % liquid) in order to account for the non-equilibrium feature.

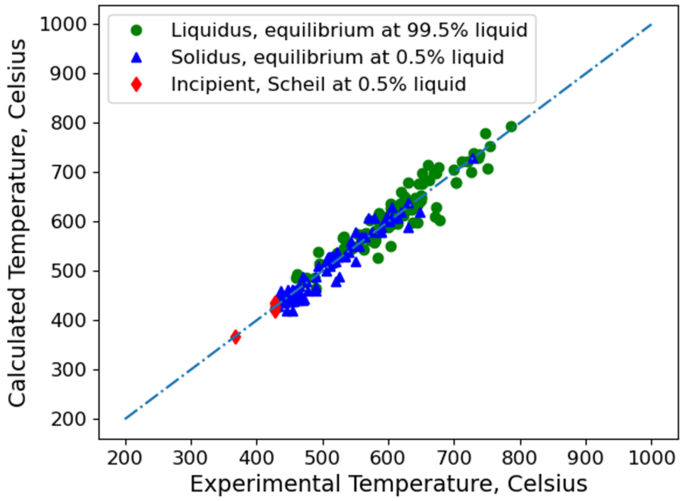

Figure 8: Comparison of calculated vs experimental liquidus temperatures and solidus temperatures, as well as incipient melting temperatures, for Mg alloys.

Tips for Analyzing Scheil Solidification Simulations

AZ91 is a series of the most important die casting Mg alloys. Using the TCS Mg-based Alloys Database (TCMG), you can simulate the solidification process of the AZ91 alloy using Scheil calculations.

Read more about Scheil Solidification Simulations on our website, including how to select the right model for your simulation. If you are in Thermo-Calc, press F1 to search the help to learn about using Scheil.

The typical microstructures of the solidified AZ91 alloys usually consist of (Mg) grains and mainly the $Al_{12}Mg_{17}$ phase at the grain boundaries [2006Wan; 2009Kab]. Similar microstructures are observed in other AZ series alloys [2011Wu].

The following suggestions are useful to help you analyze the simulated results and interpret experimental observations.

When working in Thermo-Calc with Scheil simulations, you use either the Scheil Calculator (in Graphical Mode) or the Scheil module (in Console Mode). The fundamental calculation engine is the same but you access the settings in different ways.

Check the Calculated Phase Fractions

It is recommended to always check the calculated phase fractions in your results before comparing the simulation with experimentally observed microstructures.

The following example uses an alloy composition of 8.82 wt. % Al, 0.91 wt. % Zn, 0.31 wt. % Mn, Mg balance. Figure 9 plots the total fraction of solid phases against temperature from the solidification calculation of an AZ91 alloy.

The calculation predicts the formation of three Al-Mn compounds, Al_8Mn_5, $Al_{11}Mn_4$, and Al_4Mn, in addition to the experimentally observed phases, HCP_A3-(Mg) and $Al_{12}Mg_{17}$. At first glance, the prediction of phase formation is obviously different from the experimental observations.

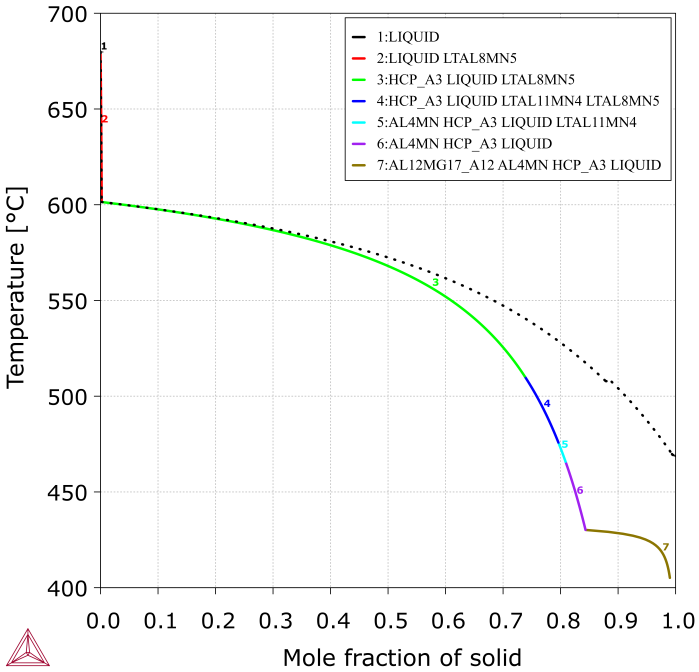

Figure 9: Scheil solidification with all the phases included and the total fraction of solid phases against temperature. The solid line corresponds to the Scheil calculation and the dashed line to the equilibrium calculation.

However, when you compare this to Figure 10, the amounts of the Al-Mn compounds are negligible. Of these, Al_8Mn_5 has the highest amount but less than 0.3% and the other two are less than 0.01%.

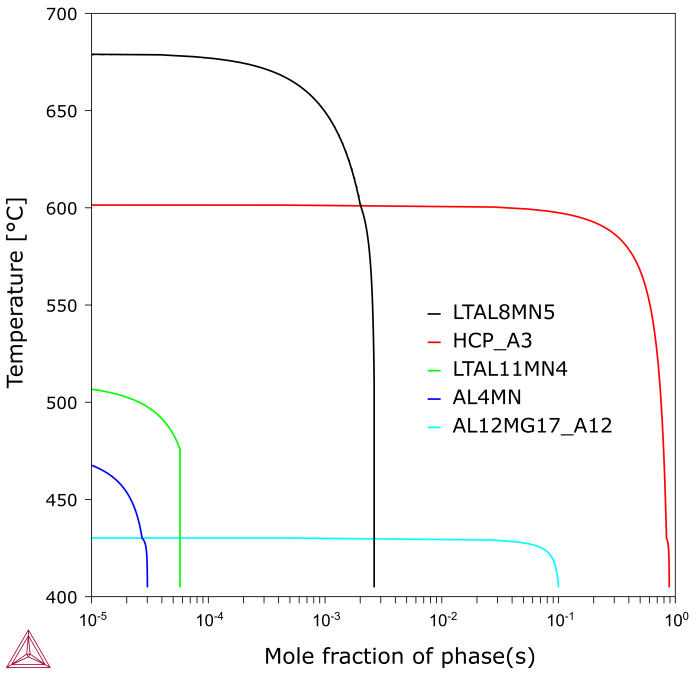

Figure 10: Scheil solidification with all the phases included and the Al-Mn compounds are in negligible amounts.

The negligible amounts may be easily overlooked in experimental examination due to the small value. Especially, the Al_8Mn_5 phase forms in prior to (Al) and it would probably not appear at grain boundaries.

You can always choose to neglect the discrepancies or plan to utilize more advanced techniques in further experimental investigations if the identification of these phases is important.

Add Mn as an Alloying Element

Mn is usually added as an alloying element in Mg-Al based alloys (including AZ, AM, and AS series). This element is believed to be able to increase resistance against corrosion and prevent soldering in high-pressure die casting of magnesium alloys. Furthermore, Al_8Mn_5 usually forms at the beginning of the solidification of the AZ series Mg alloys and it had been reported that this phase might act as potent nucleation sites for (Mg). Although this ability of Al_8Mn_5 was doubted by the work of Wang et al. [2010Wan], this phase does precipitate in the solidified microstructures, which confirms the present simulation. It is not easy to experimentally identify the manganese aluminides in Al-Mg based alloys, especially $Al_{11}Mn_4$ [2004Bar] and Al_4Mn [2004Dhu].

You can observe that using the TCS Mg-based Alloys Database (TCMG) the Scheil simulation agrees with experimental observations. Further, the theoretical calculations can predict the phases that have a minor or trace amount, which are otherwise difficult to experimentally identify.

Reject Phases with Negligible Amounts

Practically, during the simulation you can reject the phases that have negligible amounts.

It can be distracting to include insignificant phases in diagrams. Practically, you can do a second-round simulation excluding those phases. This is accomplished by first rejecting all phases and then restoring those of interest.

The following example uses the same alloy composition as in the previous examples, 8.82 wt. % Al, 0.91 wt. % Zn, 0.31 wt. % Mn, Mg balance. Figure 11 shows the simulated Scheil solidification curve with only liquid, Al_8Mn_5, HCP_A3 and $Al_{12}Mg_{17}$ included. The solidification curve is almost the same as that in Figure 9 as is the phase formation of the major phases. However, with those minor phases excluded it is much easier to analyze the simulated results.

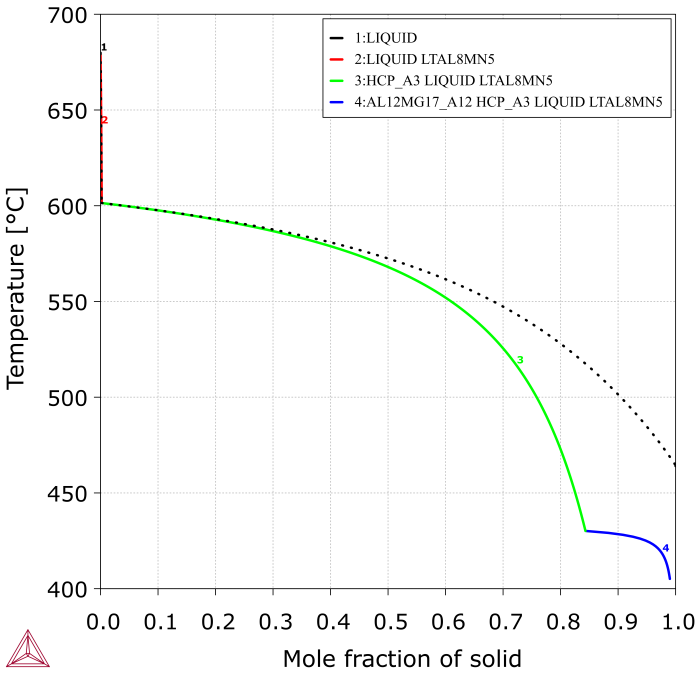

Figure 11: Scheil solidification of the AZ91 alloy with only Liquid, Al8Mn5, Hcp_A3, and Al12Mg17 included.

Adjust the Minor Alloying Elements

In a simulation, you can exclude or include some of the minor alloying elements that have no significant effects on the solidification sequence.

Instead of rejecting the minor phases during the set up of your solidification simulation, you can also exclude some of the minor alloying elements that have no significant effects on the solidification sequence. This is particularly useful when the alloy contains a large number of alloying elements and when many intermetallic phases may potentially form. In the case of the AZ91 alloy, you can consider excluding Mn in the simulation. This has the advantage of getting rid of all the Mn-bearing compounds including Al_8Mn_5.

However, whether to include or exclude a minor alloying element depends on the purpose of the simulation. For example, sometimes it is important to know the impact of impurities on solidification and formation of the primary phase.

Figure 12 shows a Scheil simulation of an AZ91D alloy by considering a small amount (about 0.15 wt.%) of Fe impurity. The solidification starts with the formation of B2-AlFe, followed by Al_8Mn_5. It was experimentally observed by [2018Zen] that Al_8Mn_5 actually nucleated on the B2 phase. In this case, the impurity, Fe, as well as the minor alloying element, Mn, has to be considered in order to account for the experimental observations.

Interpret the Thermal Analysis Data

It is useful to spend time interpreting the thermal analysis data.

Al_8Mn_5 is the primary phase during the solidification of the AZ91 alloy. The liquidus temperature (i.e. the start of the solidification of Al_8Mn_5) is calculated to be 680 °C.

The first arrested thermal effect in some thermal analysis experiments, e.g., 600.6 °C [2014Bak] or 604 °C [2004Rid], does not correspond to the liquidus temperature, but is related to the start of the solidification of (Mg), which is 601.4 °C according to the Scheil calculation.

Since the amount of Al_8Mn_5 is low, the heat effect corresponding to the solidification of Al_8Mn_5 is too small to be readily detected. Precisely conducted thermal analysis, however, can still detect the thermal effect. Thorvaldsen and Aliravci [1992Tho] successfully measured the Al_8Mn_5 liquidus in several AZ91 alloys with 9.1 wt. % Al, 1.53 wt. % Zn and Mn varying from 0 to 1 wt.%. It has been shown in (in calculation examples) that these data can be well accounted for by the phase diagram calculated using the TCS Mg-based Alloys Database (TCMG).

Experimental Techniques and Back Diffusion

It is recommended to make moderate use of Scheil solidification since a real solidification is expected to be between a Scheil solidification simulation and an equilibrium solidification simulation.

The Scheil solidification simulation provides a good approximation to non-equilibrium solidification processes and is widely used. However, it should be noted that any experimental technique has disadvantages and blind spots. Since transition temperatures are often measured with thermal analysis, the heat effect must be significant enough to be detected. Although it is well-known, as predicted here, the primary phase in AZ91 alloys is Al_8Mn_5, but its amount is too small to be detected. The liquidus temperature was measured to be 603.5 °C [2004Rid], in comparison with 680 °C as predicted in the Scheil simulation in Figure 12. However, the seemingly different results actually imply a good agreement. The experimental temperature actually corresponds to the start precipitation of (Mg) grains, i.e. HCP_A3, where the thermal effect became noticeable. The agreement is very good. Therefore, one has to understand how the results were measured and what could make a difference, while comparing the results with the simulations.

Figure 12 also shows the solidification curve derived from thermal analysis. A good agreement was seen between the experimental results and the Scheil simulation in the early stage. When the solid fraction is larger than 50%, however, there is a noticeable or significant difference. Such experimental results should be considered qualitative, since quite a few assumptions are made during the derivation, for example, that (1) the heat is proportional to the solid phase fraction and (2) the heat transfer is immediate. Many factors may add to the uncertainties.

It should be pointed out that, conventional Scheil simulation also has its own limitation, which is the assumption that the diffusion in solid phases is negligible. Although this is reasonable in many cases, back diffusion in solid phases might sometimes become noticeable either in systems where diffusion is relatively fast or during slow cooling. In Thermo-Calc you can take the impact of back diffusion into account, as shown in Figure 12, which includes the results from a Scheil simulation with back diffusion. It results in a good agreement with the experimental solidus temperature, as well as the late solidification stage [2004Rid], although the intermediate range almost remains the same. As above, the experimental solidification curve can only be considered qualitative.

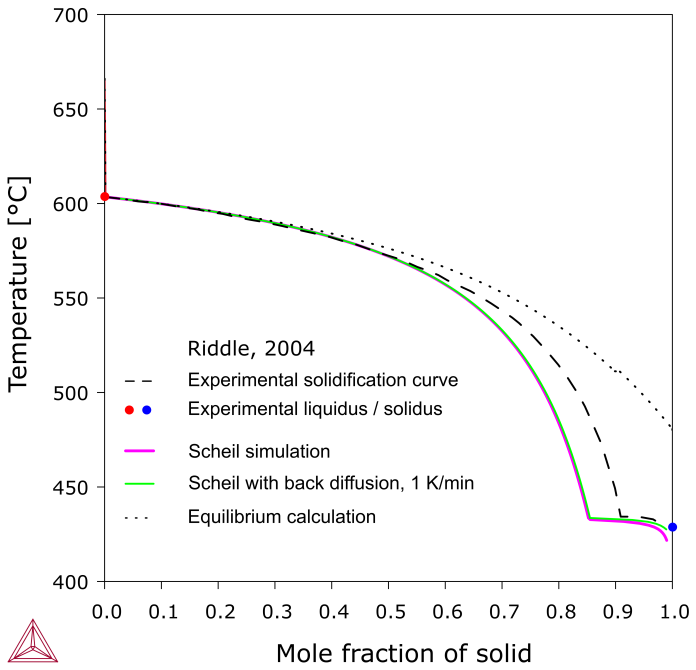

Figure 12: Comparison of the simulated equilibrium and Scheil solidification profiles with experimental thermal analysis [2004Rid].

The alloy composition used in this example is 8.7 wt. % Al, 0.5 wt. % Zn, 0.26 wt. % Mn, Mg balance.

As expected, the experimental profile is located between the two solidification simulations, while it can be better approximated with the Scheil simulation. The start temperature of the solidification of (Mg) and the eutectic temperature of L = (Mg) + $Al_{12}Mg_{17}$, together with the profile shape, are all accounted for by the Scheil simulation. However, the solid fractions from the Scheil simulation and the experiment do not agree well with each other in the region between 60% and 90%. This deviation indicates that the diffusion in the solid phases is not negligible (as assumed in Scheil) even though it is truly slow.

A real solidification process could much more approach to either of the two solidification simulations and deviate from the other, depending on the experimental conditions and the alloy systems. In order to account for the differences between the simulation and the experimental observation, you should consider the effect of back diffusion in a Scheil simulation.

References

[1992Tho] A. Thorvaldsen, C. A. Aliravci, Adv. Prod. Fabr. Light Met. Met. Matrix Comp., in Proceedings of the International Symposium, p. 277 (1992).

[2004Bar] L. P. Barber, Characterization of the solidification behavior and resultant microstructures of Magnesium-Aluminum alloys, Master's thesis, Worcester Polytechnic Institute, Worcester, MA (2004).

[2004Rid] Y. W. Riddle, M. M. Makhlouf, "Characterizing solidification by non-equilibrium thermal analysis" in Magnesium Technology 2003 (TMS (The Minerals, Metals & Materials Society), 2004), pp. 101–106.

[2004Dhu] E. Dhuka, N. Lohja, H. Oettel, D. Heger, Precipitation in Mg alloy AZ61 in dependence of various heat treatments processes. Metalurgija. 10, 233–241 (2004).

[2006Wan] Y. Wang, G. Liu, Z. Fan, Microstructural evolution of rheo-diecast AZ91D magnesium alloy during heat treatment. Acta Mater. 54, 689–699 (2006).

[2009Kab] F. Kabirian, R. Mahmudi, Effects of Zirconium Additions on the Microstructure of As-Cast and Aged AZ91 Magnesium Alloy. Adv. Eng. Mater. 11, 189–193 (2009).

[2010Wan] Y. Wang, M. Xia, Z. Fan, X. Zhou, G. E. Thompson, The effect of Al8Mn5 intermetallic particles on grain size of as-cast Mg–Al–Zn AZ91D alloy. Intermetallics. 18, 1683–1689 (2010).

[2011Wu] L. Wu, F. Pan, M. Yang, J. Wu, T. Liu, As-cast microstructure and Sr-containing phases of AZ31 magnesium alloys with high Sr contents. Trans. Nonferrous Met. Soc. China. 21, 784–789 (2011).

[2014Bak] D. P. Bakke, D. H. Westengen, “The Role of Rare Earth Elements in Structure and Property Control of Magnesium Die Casting Alloys” in Essential Readings in Magnesium Technology (Wiley, Hoboken, NJ, USA, 2014), pp. 313–318.

[2018Zen] G. Zeng, J. W. Xian, and C. M. Gourlay, Nucleation and growth crystallography of Al8Mn5 on B2-Al(Mn,Fe) in AZ91 magnesium alloys, Acta Mater., vol. 153, pp. 364–376 (2018).

Electrical Resistivity of Mg-Ag and Mg-Ce

The thermophysical properties available with the TCS Mg-based Alloys Database (TCMG) include electrical resistivity.

For more information about the various thermophysical, thermomechanical, and properties models, and when in Thermo-Calc, press F1 to search the online help. The details are found under a *General Reference* section.

You can find information on our website about the properties that can be calculated with Thermo-Calc and the Add-on Modules. Additional resources are added on a regular basis so keep checking back or subscribe to our newsletter.

Mg-Ag

The calculated electrical resistivity of Mg-Ag solution versus the Ag concentration, in comparison with the experimental data reported by Salkovitz et al. [1957Sal].

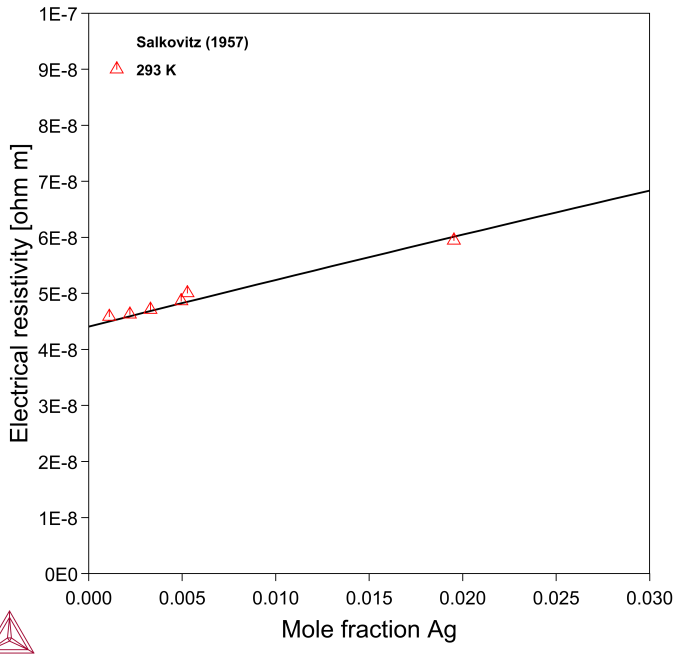

Figure 13: Calculated electrical resistivity of Mg-Ag HCP_A3 solid solution compared to experimental data from [1957Sal].

Mg-Ce

This example shows the calculated electrical resistivity of Mg-Ce solution versus the temperature, on which the data measured by Powell et al [1964Pow] are imposed.

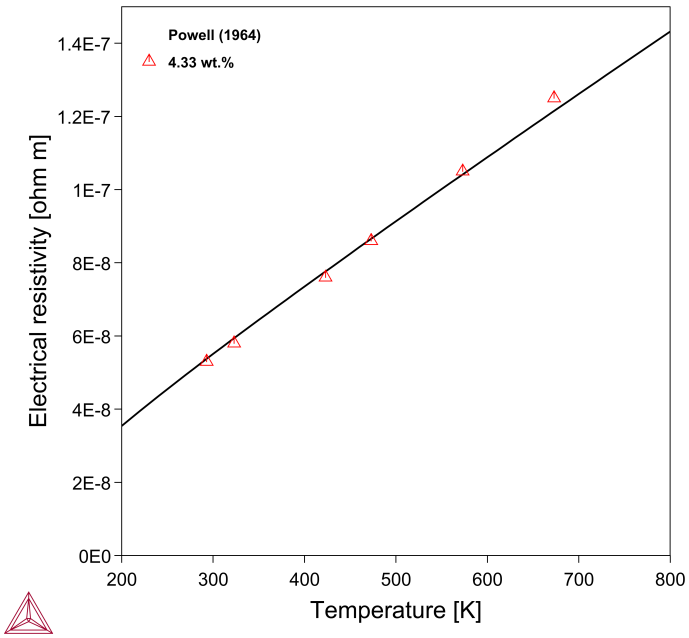

Figure 14: Calculated electrical resistivity of Mg-Ce HCP_A3 solid solution compared to experimental data from [1964Pow].

References

[1957Sal] E. I. Salkovitz, A. I. Schindler, E. W. Kammer, Transport Properties of Dilute Binary Magnesium Alloys. Phys. Rev. 105, 887–896 (1957).

[1964Pow] R. W. Powell, M. J. Hickman, R. P. Tye, The thermal and electrical conductivity of magnesium and some magnesium alloys. Metall. Br. J. Met. 70, 159–163 (1964).

Thermal Conductivity of Mg-Gd, Mg-Y, and Mg-Gd-Y

The thermophysical properties available with the TCS Mg-based Alloys Database (TCMG) include thermal conductivity.

For more information about the various thermophysical, thermomechanical, and properties models, and when in Thermo-Calc, press F1 to search the online help. The details are found under a *General Reference* section.

You can find information on our website about the properties that can be calculated with Thermo-Calc and the Add-on Modules. Additional resources are added on a regular basis so keep checking back or subscribe to our newsletter.

Mg-Gd

The thermal conductivity of Gd-Mg alloys was measured in two papers [201Zho and 2019Hua] with solution treated alloys (at 798 K for 24 hours or 673 K for 30 days, respectively). Some of the alloys are expected to consist of fully (Mg) solid solution while some contain also the intermetallic compound Mg_5Gd. Figure 15 shows the calculated thermal conductivity of (Mg) at different Gd concentrations versus the temperature in comparison with the single-phase data from Huang [2019Hua].

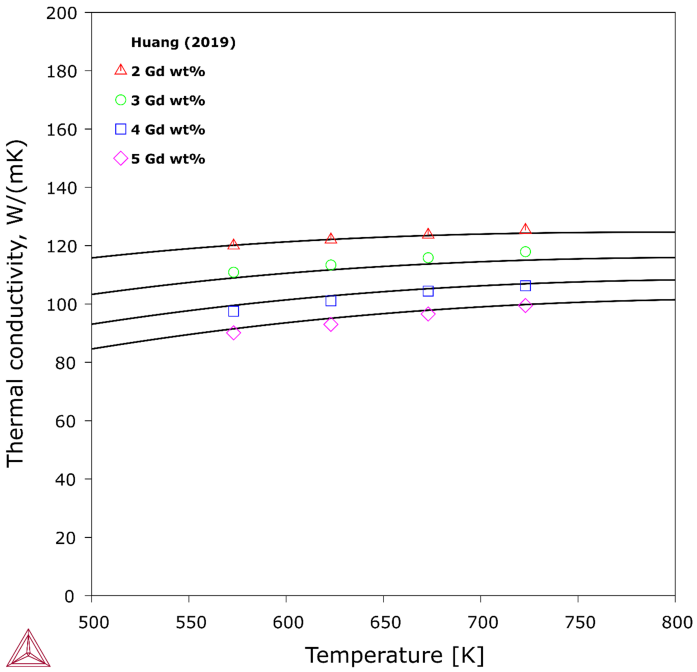

Figure 15: Calculated thermal conductivity of HCP_A3 solution in the Mg-Gd system, versus the temperature.

Figure 16 re-plots the thermal conductivity of (Mg) solid solution versus the composition of Gd, based on the recent experimental investigation by Huang [2019Hua] as well as considering results from Zhong et al. [2017Zho].

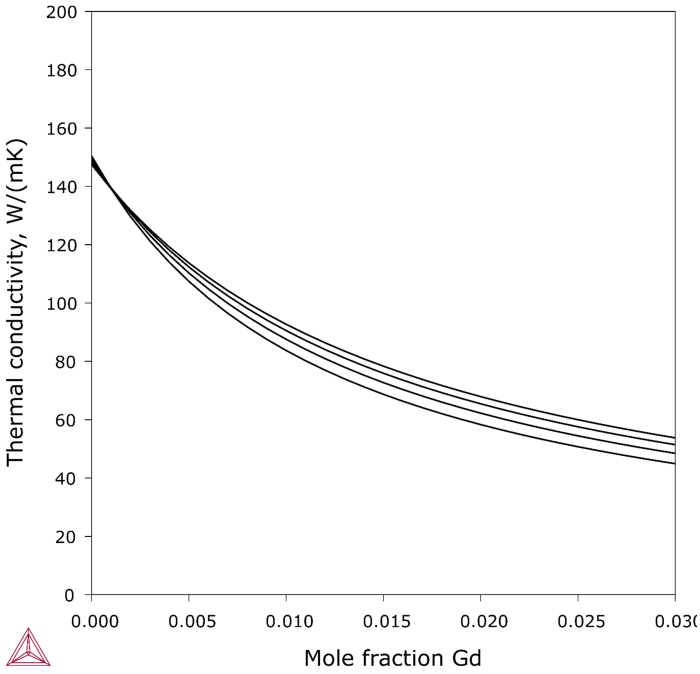

Figure 16: Calculated thermal conductivity of HCP_A3 solution in the Mg-Gd system, versus the Gd content.

Mg-Y

Zhong et al. [2017Zho], Huang [2019Hua], and Su et al. [2018Su] recently measured thermal conductivity of Mg-Y solution with heat-treated alloys. The heat treatments were performed, respectively, at 525 °C for 12 h, 400 °C for 30 days, and at 530 °C for 12 h. The two datasets by Zhong [2017] and Su [2018] generally agree with each other, but the former does not reasonably extrapolate to pure Mg, as shown in Figure 17. Interestingly, the datasets from Huang [2019] and Su et al. [2018] both extrapolate reasonably to pure Mg, although they differ noticeably from each other. The current description was derived mainly with the data from [2018Su] but with a compromise on a slightly better fitting to the data by [2019Hua].

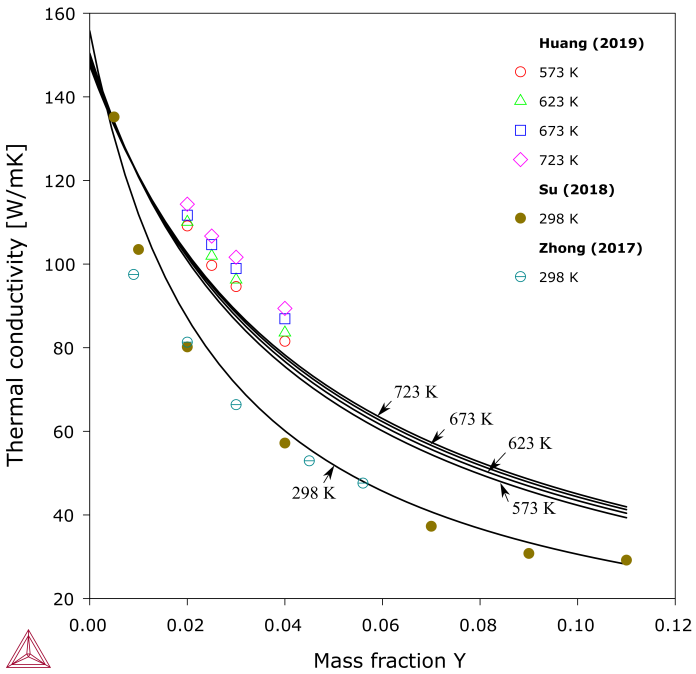

Figure 17: Calculated thermal conductivity of the HCP_A3 Mg-Y solid solution.

Mg-Gd-Y

With the Gd-Mg and Mg-Y descriptions, the thermal conductivity of Mg-Gd-Y HCP_A3 solid solution can be reasonably extrapolated. As shown in Figure 18, the calculations well agree with the data by Huang [2019]. It is worth noting that no ternary interaction is used to avoid overfitting. The agreement with the ternary data also indicates that the binary Mg-Y data by Huang [2019] might be overestimated.

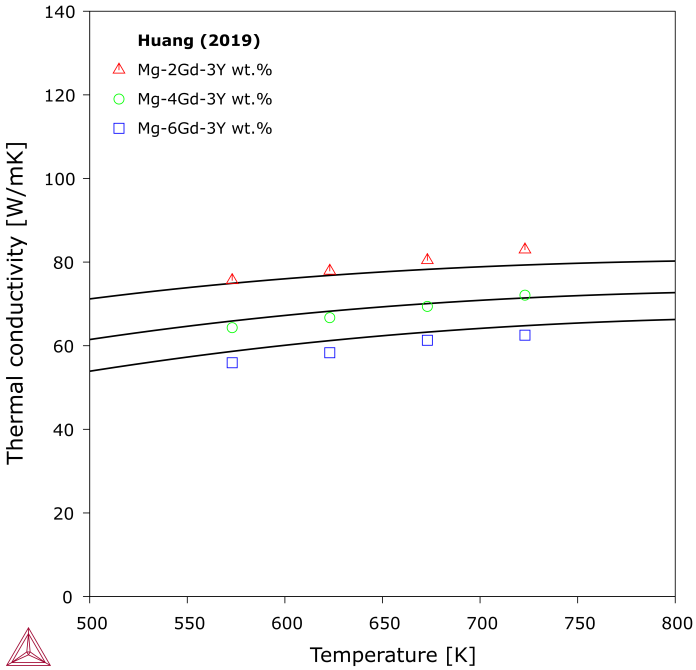

Figure 18: Calculated thermal conductivity of Mg-Gd-Y HCP_A3 solid solution.

Zhong et al. [2017Zho] also reported thermal conductivity data from as-cast alloys. There are two aspects that need to be considered:

- The extra phases that form in the alloys in additional to the HCP_A3 (Mg) solid solution.
- The compositions segregation, especially in the (Mg) solution.

In order to account for such data, the calculations are done based on a series of Scheil simulations on various alloy compositions. From each simulation, the volume fraction of each layer of solid that forms at each (temperature) step of the solidification simulation is evaluated. Also evaluated is the thermal conductivity of each layer at the measuring temperature (room temperature in this case) according to the freeze-in concept. Then we sum up the quantities of all layers according to the volume fractions to predict the quantity for the whole as-cast alloy at the measuring temperature. This routine is repeated for a series of composition to get the curve shown in the plot.

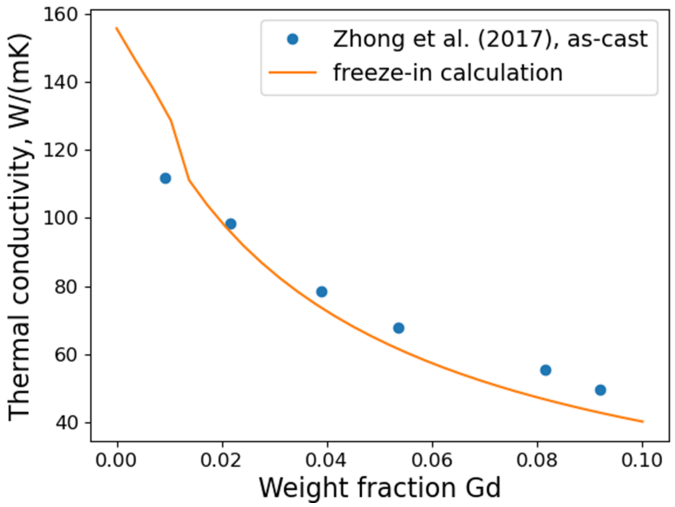

Figure 19: Predicted thermal conductivity compared to as-cast experimental data from [2017Zho]. This plot is created using a custom TC-Python script, based on a series of Scheil simulations with TC-Python.

References

[2017Zho] L. Zhong, J. Peng, S. Sun, Y. Wang, Y. Lu, F. Pan, Microstructure and Thermal Conductivity of As-Cast and As-Solutionized Mg–Rare Earth Binary Alloys. J. Mater. Sci. Technol. 33, 1240–1248 (2017).

[2018Su] C. Su, D. Li, A. A. Luo, T. Ying, X. Zeng, Effect of solute atoms and second phases on the thermal conductivity of Mg-RE alloys: A quantitative study. J. Alloys Compd. 747, 431–437 (2018).

[2019Hua] L. Huang, Experimental measurement and computational simulation of thermal conductivity of Mg-Al-Zn and Mg-Gd-Y system, Central South University, Master's thesis (2019).

Viscosity of AZ91D and AZ31 Alloys

The viscosity thermophysical property data is included with the TCS Mg-based Alloys Database (TCMG) starting with version 6 (TCMG6).

For more information about the various thermophysical, thermomechanical, and properties models, and when in Thermo-Calc, press F1 to search the online help. The details are found under a *General Reference* section.

You can find information on our website about the properties that can be calculated with Thermo-Calc and the Add-on Modules. Additional resources are added on a regular basis so keep checking back or subscribe to our newsletter.

AZ91D

Kinematic viscosity of AZ91D alloy has been measured in several studies [2006Par; 2008Aba; 2009Mi] but the results of these measurements are not in agreement with each other. This plot shows the viscosity plot of AZ91D alloys as a function of temperature along with the experimental data.

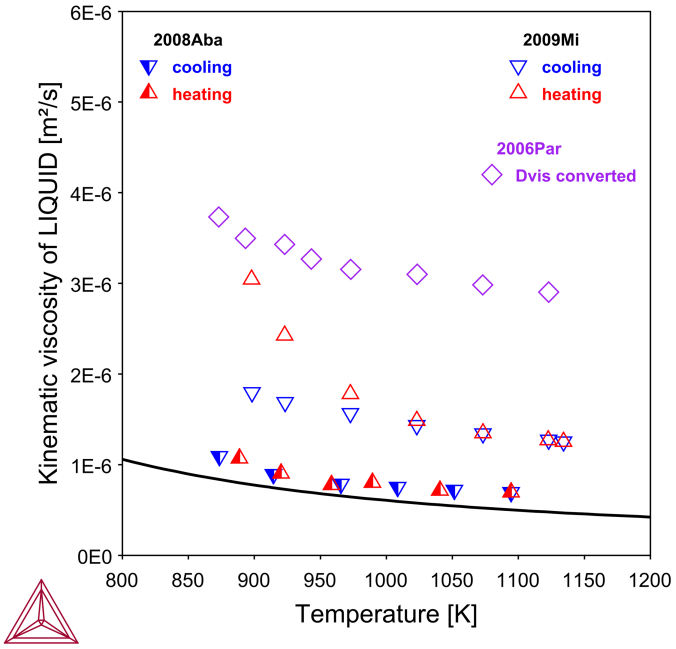

Figure 20: Calculated kinematic viscosity of AZ91D alloy.

AZ31

The following figure shows the comparison between the measured and calculated values of the dynamic viscosity of the AZ31 alloy.

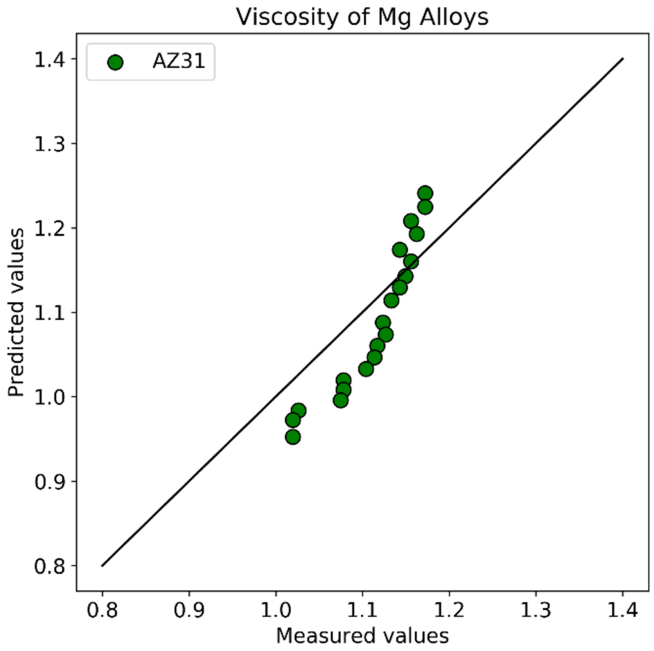

Figure 21: Predicted values of the dynamic viscosity of AZ31 is compared with the measured data. The experimental data is taken from [2013Yak].

References

[2006Par] S. H. Park, B. Y. Hur, “Surface tension and viscosity of Mg alloys” in Institute of Cast Metals Engineers - 67th World Foundry Congress, Wfc06: Casting the Future (Institute of Cast Metals Engineers (ICME), Harrogate, UK, 2006)vol. 1, pp. 288–294.

[2008Aba] I. S. Abaturov, P. S. Popel, I. G. Brodova, V. V Astafiev, L. Peijie, Exploration of the viscosity temperature dependences and microstructure of magnesium-based commercial alloy AZ91D with small additions of calcium. J. Phys. Conf. Ser. 98, 062023 (2008).

[2009Mi] G. Mi, L. He, L. Pei-jie, P. S. Pope, I. S. Abaturov, Viscosity of AZ91D magnesium alloy melt with small additions of calcium. Chinese J. Nonferrous Met. 19, 1372–1378 (2009).

[2013Yak] A. Yakymovych, Y. Plevachuk, V. Sklyarchuk, “Influence of Zn and Al additions on viscosity of liquid Mg” in Magnesium Technology 2013 (Montreal, Canada, 2013), pp. 1600–1605.

TCMG Calculation Examples

Some diagrams are calculated with earlier versions of the database. Negligible differences might be observed if these are recalculated with the most recent version. The diagrams are updated when there are considerable or significant improvements.

In this section:

Binary Phase Diagrams

You can use the TCS Mg-based Alloys Database (TCMG) to plot binary phase diagrams in Thermo-Calc. These examples show a selection of the important assessed systems that are the building blocks of the database itself when applying the CALPHAD method.

Learn more on our website about the CALPHAD Method and how it is applied to the Thermo-Calc databases. Also visit the video tutorials on our website or our YouTube playlist.

When working in Thermo-Calc with binary diagrams you use either the Binary Calculator (in Graphical Mode) or the Binary module (in Console Mode). The fundamental calculation engine is the same but you access the settings in different ways.

Al-Mg

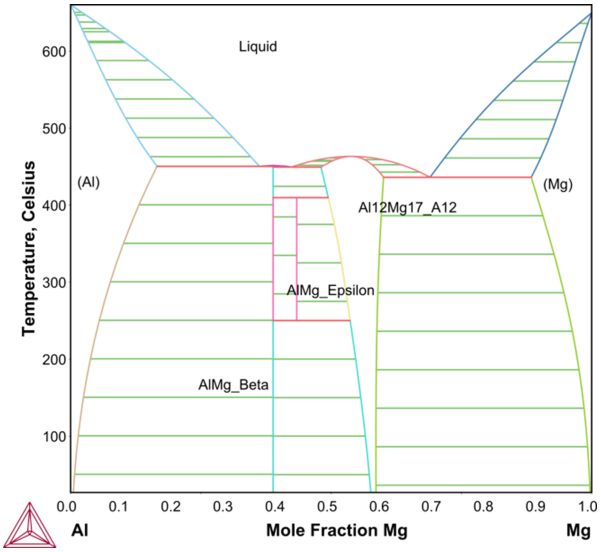

Figure 22: Calculated Al-Mg phase diagram [1998Lia].

Gd-Mg

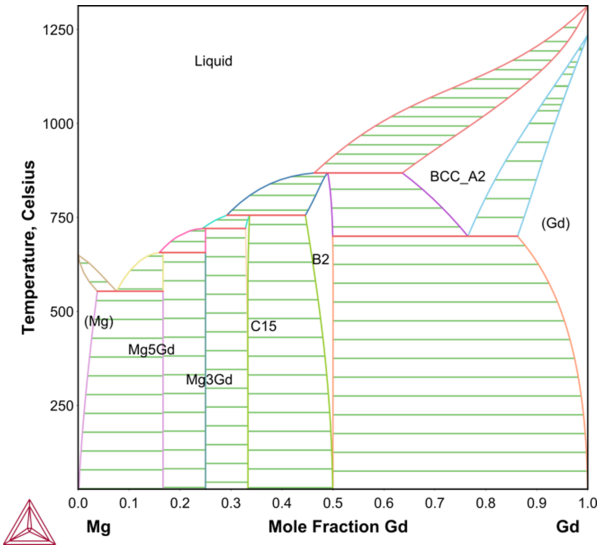

Figure 23: Calculated Gd-Mg phase diagram [2007Guo].

Ho-Mg

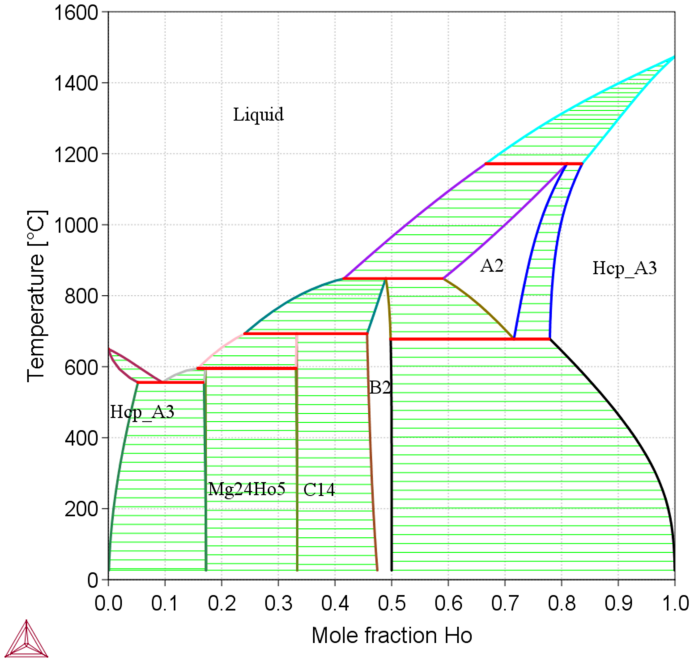

Figure 24: Calculated Ho-Mg phase diagram [2018Che].

Dy-Mg

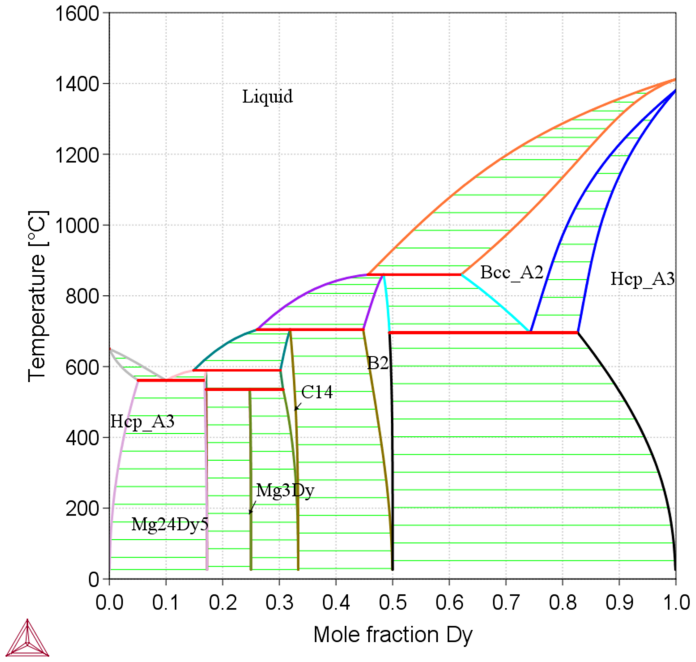

Figure 25: Calculated Dy-Mg phase diagram [2018Che].

In-Mg

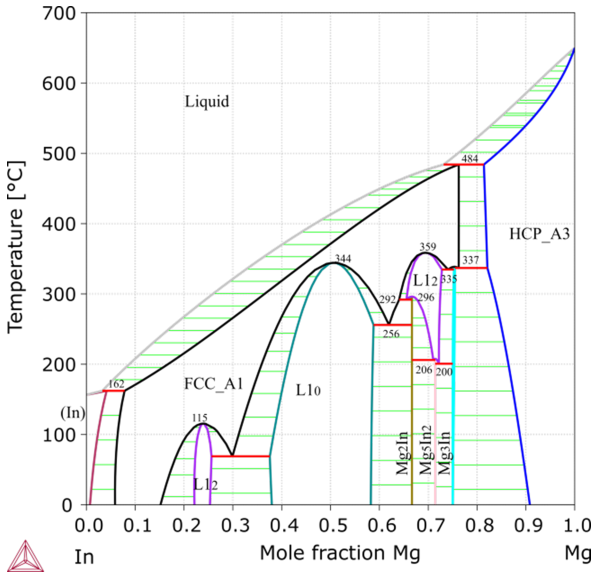

Figure 26: Calculated In-Mg phase diagram [2018Che].

References

[1998Lia] P. Liang, H.-L. Su, P. Donnadieu, M. G. Harmelin, A. Quivy, P. Ochin, G. Effenberg, H. J. Seifert, H. L. Lukas, F. Aldinger, Experimental investigation and thermodynamic calculation of the central part of the Mg-Al phase diagram. Zeitschrift für Met. 89, 536–540 (1998).

[2007Guo] C. Guo, Z. Du, C. Li, A thermodynamic description of the Gd–Mg–Y system. Calphad. 31, 75–88 (2007).

[2018Che] H.-L. Chen, Modeling of Mg-Ag, Mg-Dy, Mg-Er, Mg-Ho, Mg-In, Ag-In, Al-In, Ce-In, Gd-In, In-K, In-Li, In-Mn, In-Na, In-Nd, In-Ni, In-Pr, In-Sc, In-Th, In-Y and In-Zr binary system in TCMG5, Thermo-Calc Software (2018).

Ternary Phase Diagrams

You can use the TCS Mg-based Alloys Database (TCMG) to plot ternary phase diagrams in Thermo-Calc. These examples show a selection of the important assessed systems that are the building blocks of the database itself when applying the CALPHAD method.

Learn more on our website about the CALPHAD Method and how it is applied to the Thermo-Calc databases. Also visit the video tutorials on our website or our YouTube playlist.

When working in Thermo-Calc with ternary diagrams you use either the Ternary Calculator (in Graphical Mode) or the Ternary module (in Console Mode). The fundamental calculation engine is the same but you access the settings in different ways.

Mg-Gd-Zn

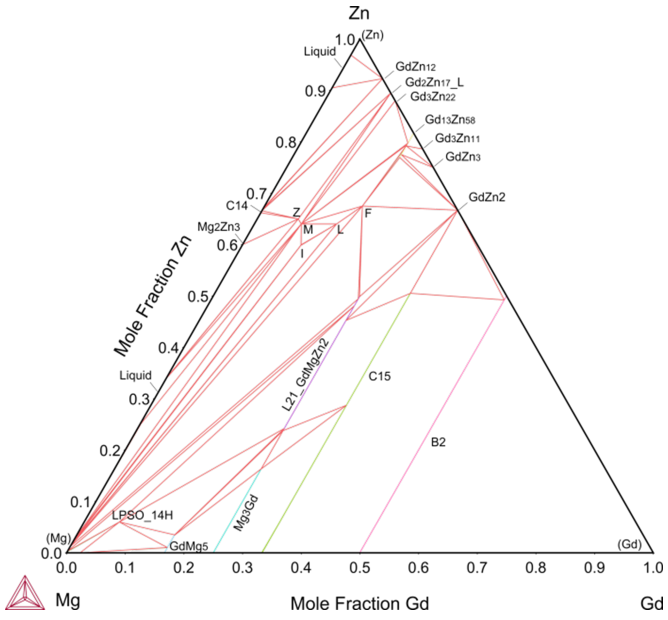

Figure 27: Calculated Mg-Gd-Zn phase equilibria at 673 K [2015aChe].

Al-Li-Mg

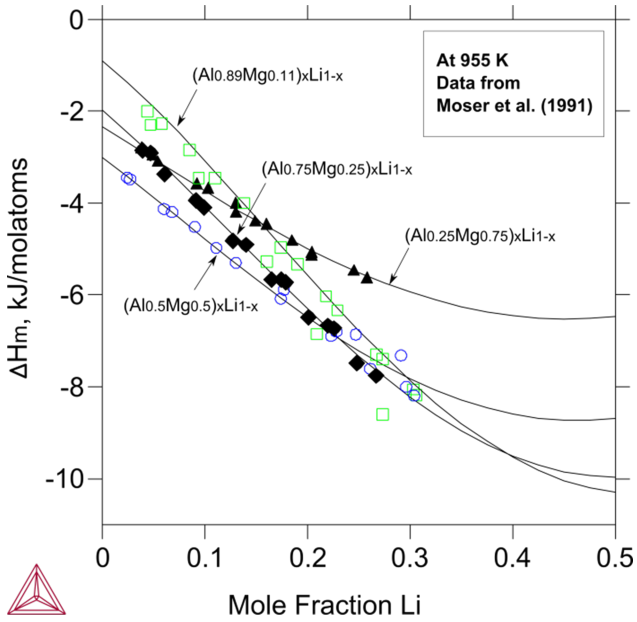

Figure 28: Calculated enthalpy of mixing of liquid at 955 K along several compositional lines in the Al-Li-Mg system [2011Wan].

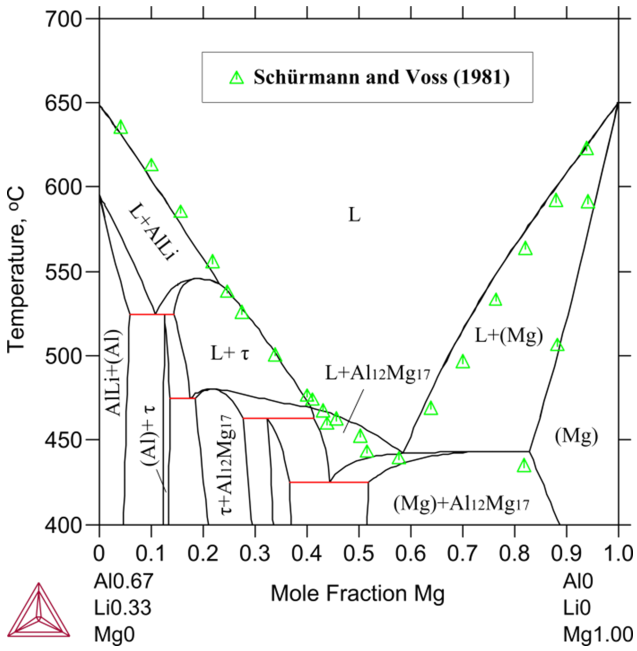

Figure 29: Calculated vertical section from Mg to $Al_{0.67}Li_{0.33}$ in the Al-Li-Mg system [2011Wan].

Gd-Mg-Nd

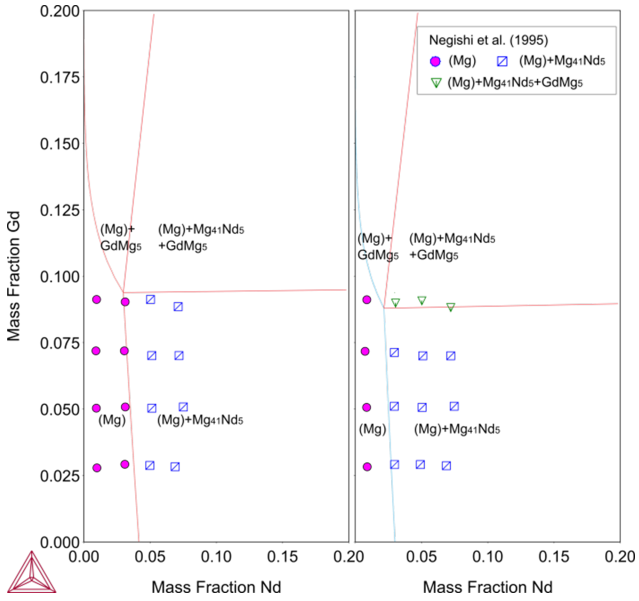

Figure 30: Calculated Mg-rich phase equilibria of the Gd-Mg-Nd system at 773 K and 808 K [2011Qi].

Cu-Mg-Y

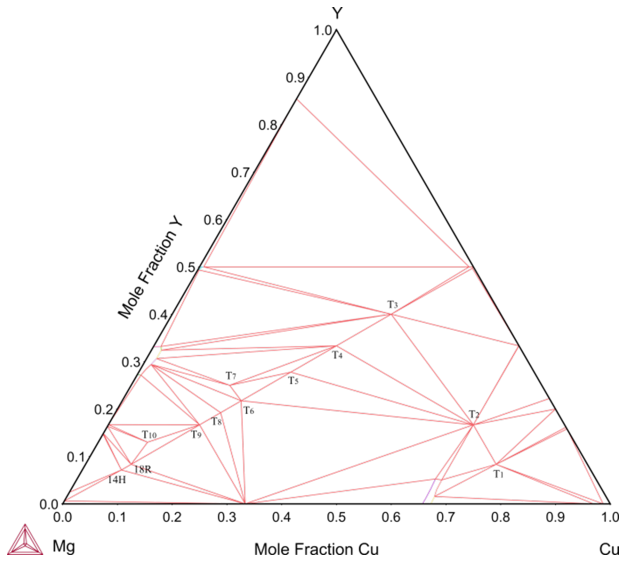

Figure 31: Calculated Cu-Mg-Y phase equilibria at 673 K [2015cChe].

Cu-In-Mg

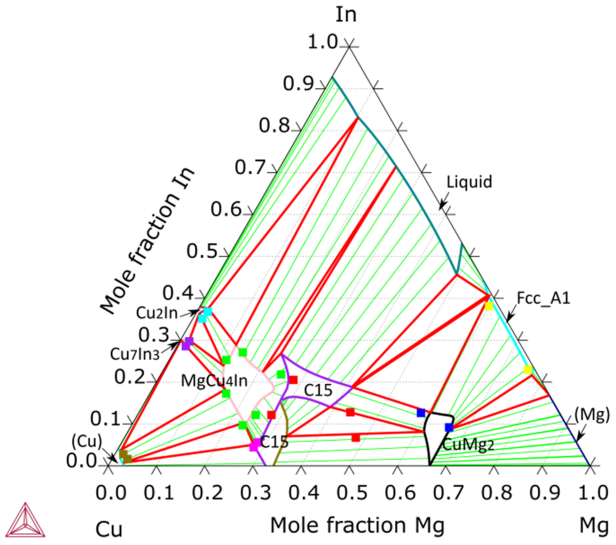

Figure 32: Calculated Cu-In-Mg phase equilibria at 673 K [2018Che].

Ag-Gd-Mg

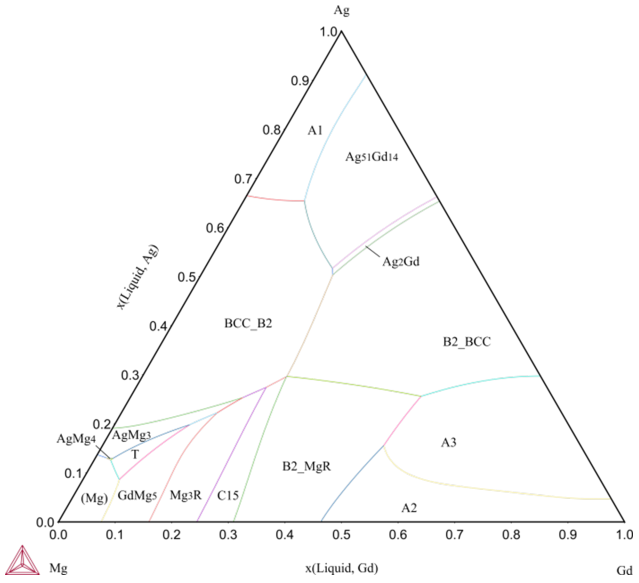

Figure 33: Calculated Ag-Gd-Mg liquidus projection [2015bChe].

References

[2008Cao] H. Cao, C. Zhang, J. Zhu, G. Cao, S. Kou, R. Schmid-Fetzer, Y. A. Chang, Experiments coupled with modeling to establish the Mg-rich phase equilibria of Mg–Al–Ca. Acta Mater. 56, 5245–5254 (2008).

[2011Qi] H.Y. Qi, Thermodynamic assessment of the Gd-Mg-Nd system, unpublished work (with modifications) (2011).

[2011Wan] P. Wang, Y. Du, S. Liu, Thermodynamic optimization of the Li–Mg and Al–Li–Mg systems. Calphad. 35, 523–532 (2011).

[2015aChe] H.-L. Chen, Thermodynamic assessment of the Gd-Mg-Zn and Mg-Y-Zn systems in TCMG4, Thermo-Calc Software (2015).

[2015bChe] H.-L. Chen, Thermodynamic assessment of the Ag-Gd-Mg system in TCMG4, Thermo-Calc Software (2015).

[2015cChe] H.-L. Chen, Thermodynamic assessment of the Cu-Mg-Y system in TCMG4, Thermo-Calc Software (2015).

[2018Che] H.-L. Chen, Thermodynamic assessment of the Cu-In-Mg system in TCMG5, Thermo-Calc Software (2018).

Mg-RE (Rare Earth) Alloy Systems

Rare earth (RE) elements are especially important to the mechanical properties of many series of magnesium alloys.

> Among the 102 ternary systems currently assessed in TCS Mg-based Alloys Database (TCMG) starting with version 6 (TCMG6), 43 systems are RE (rare earth) containing, which is about 42 % of the total number.

This section presents a few simple examples for phase equilibria calculations and solidification simulations in Mg-RE alloys. In fact, most precipitation hardenable magnesium alloys are RE-containing. All stable precipitates and important metastable ones are modeled.

The designations are not consistent. Taking the Mg-Nd system as an example, the typical sequence is: β'' ($D0_{19}$) > β'(Mg_7Nd) >> β_1 ($D0_3$) >> β ($Mg_{12}Nd$) >> βe ($Mg_{41}Nd_5$). Translational precipitates between β' and β'' are sometimes designated as β''' ($Mg_{3-7}Nd$).

Gd-Mg-Y

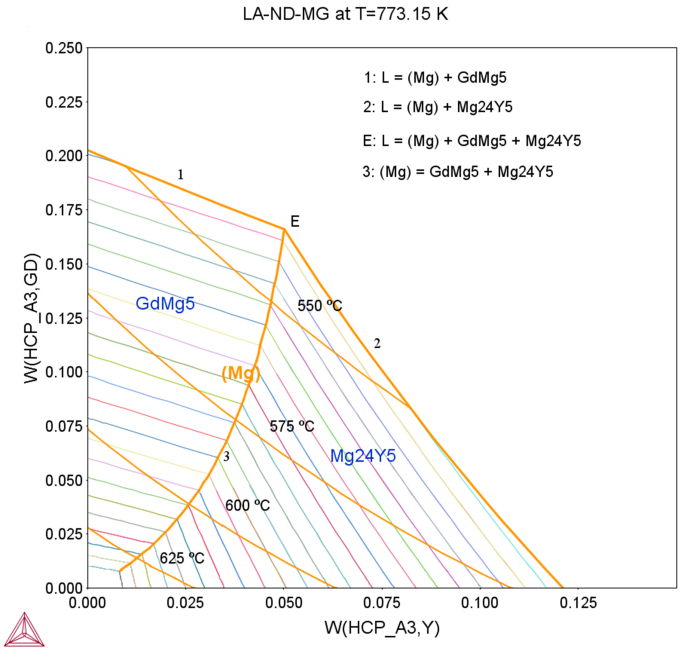

Figure 34: Calculated solidus and solvus of the (Mg) solution in the Gd-Mg-Y system [2007Guo].

Mg-Nd

Figure 35 shows the calculated (Mg) solvi, relative to various stable and metastable precipitates in the Mg-Nd binary system.

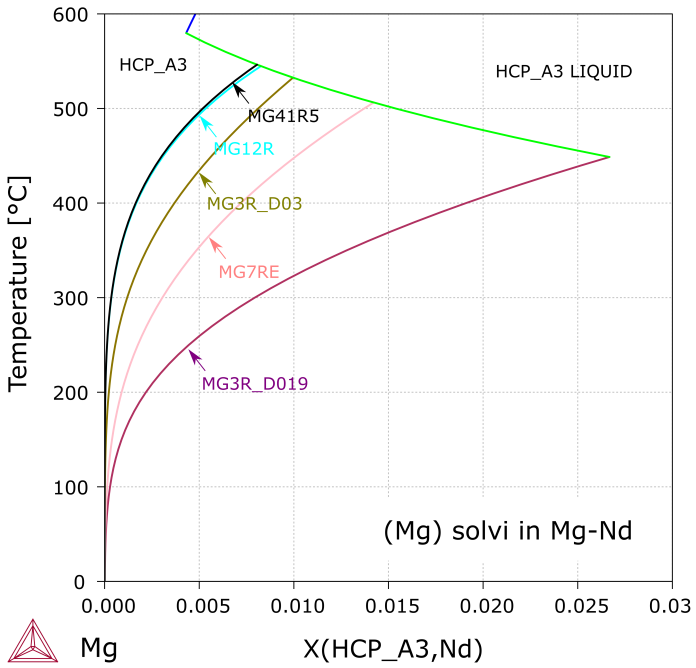

Figure 35: Calculated solvi of the (Mg) solution in the Mg-Nd binary system, relative to various stable and metastable precipitates [2020Che].

Mg-8Gd-0.6Zr-3(Nd, Y) Alloys

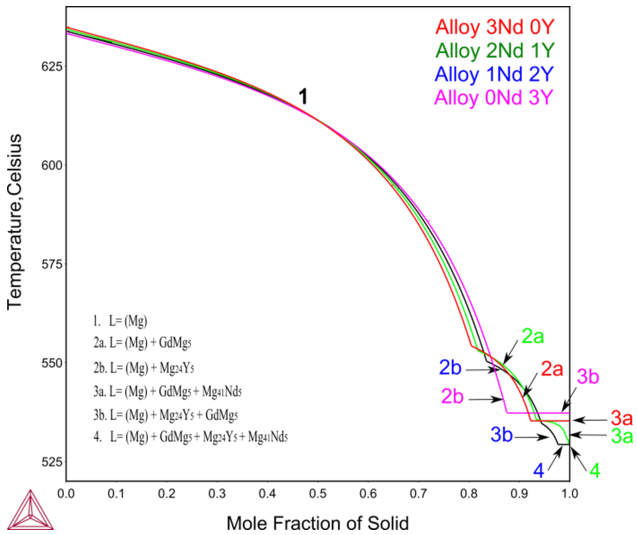

Figure 36: Scheil solidification calculations of the Mg-8Gd-0.6Zr-3(Nd, Y) alloys.

References

[2007Guo] C. Guo, Z. Du, C. Li, A thermodynamic description of the Gd–Mg–Y system. Calphad. 31, 75–88 (2007).

[2020Che] H.-L. Chen, Modeling Mg-RE (rare earth) metastable precipitates in TCMG6, Thermo-Calc Software (2020).

Ce-Mg-Nd System

Thermodynamic descriptions of core systems are of fundamental importance to the TCS Mg-based Alloys Database (TCMG). As an example, this section presents the modeling results of a core ternary system, Ce-Mg-Nd.

The modeling highlights the use of experimental data from as-cast alloys, together with those from heated alloys. Heated alloys help to determine the phase equilibria in the system, while as-cast alloys provide information on phase transition during the course of solidification although it is in general more difficult to analyze an as-cast alloy than a heated alloy.

Figure 37 shows calculated Ce-Mg-Nd isothermal section at 773 K. Figure 38 shows a calculated Ce-Mg-Nd liquidus projection, in comparison with phases observed in as-cast alloys.

The phase formation sequences in the six alloy compositions are summarized as follows.

- A and B: (Mg) > $Mg_{12}R$; C: $Mg_{12}R$ > ?; D: $Mg_{12}R$ +(Mg) ?; E: Mg_3R > $Mg_{12}R$; F: $Mg_{41}R_5$ > $Mg_{12}R$. *The question mark "?" means either uncertain or unknown.*

- The phase formation in alloys C, D, and E can be interpreted with the metastable calculation.

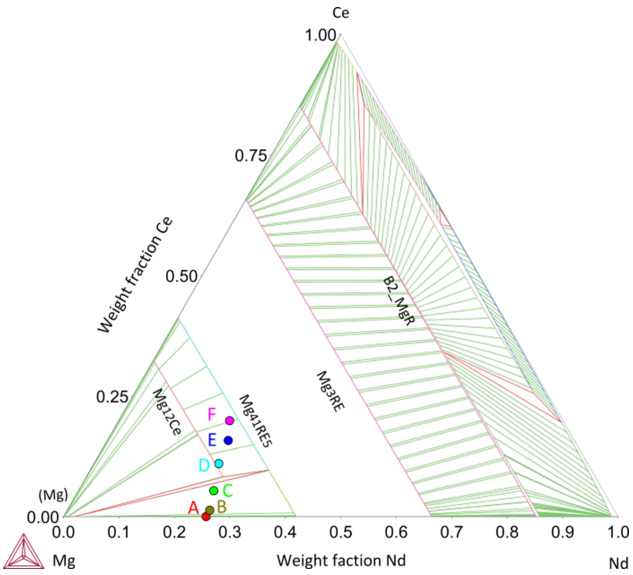

Figure 37: Calculated Ce-Mg-Nd isothermal section at 773 K. Heated alloys A, B, and C: (Mg) and $Mg_{41}R_5$; D, E, and F: $Mg_{41}R_5$ and $Mg_{12}R$.

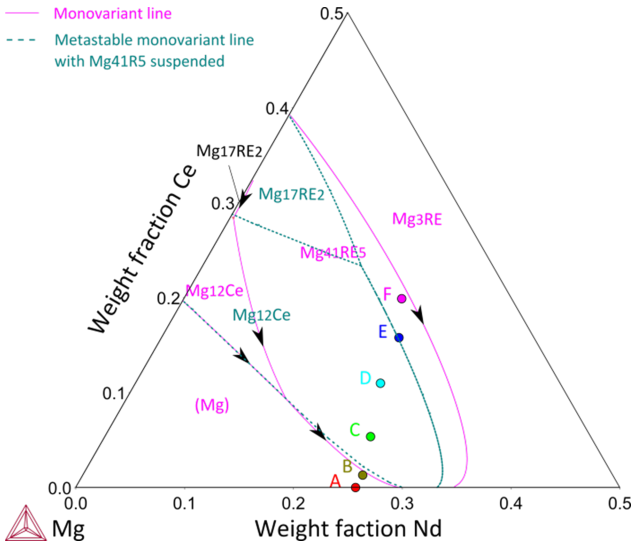

Figure 38: Calculated Ce-Mg-Nd liquidus projection [2014Che].

Reference

[2014Che] H.-L. Chen, Modeling of the Ce-Mg-Nd ternary system in TCMG3, Thermo-Calc Software (2014).

Hydrogen Storage Alloys

Magnesium and magnesium alloys have been intensively studied for decades as hydrogen storage materials. Magnesium could form MgH_2 with hydrogen. MgH_2 has a very high hydrogen storage capacity, but has obvious disadvantages in both thermodynamics and kinetics. Researchers have attempted to optimize the thermodynamic and kinetic properties of MgH_2 via various techniques, e.g. via alloying, using catalytic additives, deforming, and nanotechnology, and so forth.

As for the alloying route, investigated alloys include Mg-Ni, Cu-Mg, Mg-Nd, Ce-Mg, and La-Mg, and so forth.

In TCS Mg-based Alloys Database (TCMG) starting with version 6 (TCMG6), eight binaries (Ce-H, Cu-H, La-Zn, H-La, H-Mg, H-Nd, H-Ni, and H-Zn) and five ternaries (Ce-H-Mg, Cu-H-Mg, H-La-Mg, H-Mg-Nd, and Mg-H-Ni) are modeled for application to hydrogen storage. This is in to the relevant systems already modeled in versions TCMG5 and earlier.

Cu-Mg-H

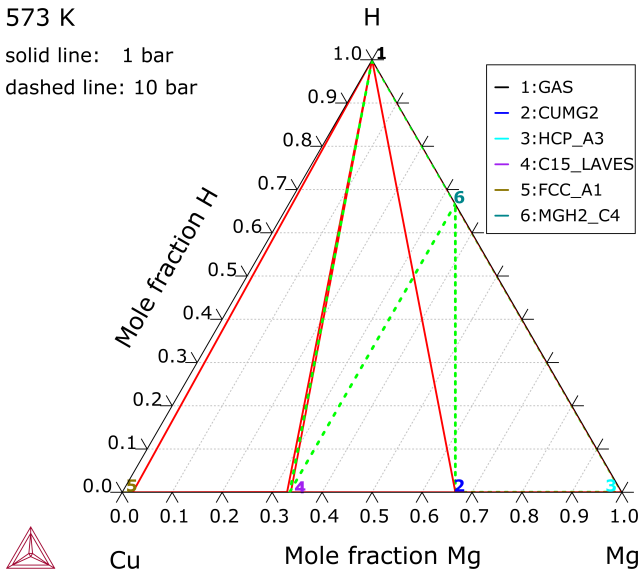

Figure 39: Calculated Cu-H-Mg isothermal sections at 573 K at different pressures [2020aChe].

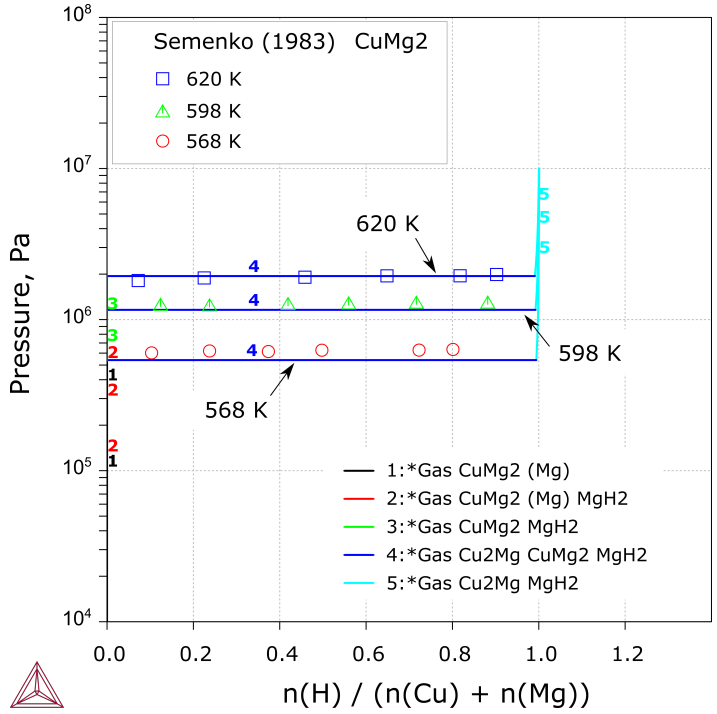

Figure 40: Calculated hydrogen dissolution pressure of a Cu-Mg_2 single-phase alloy [2020aChe].

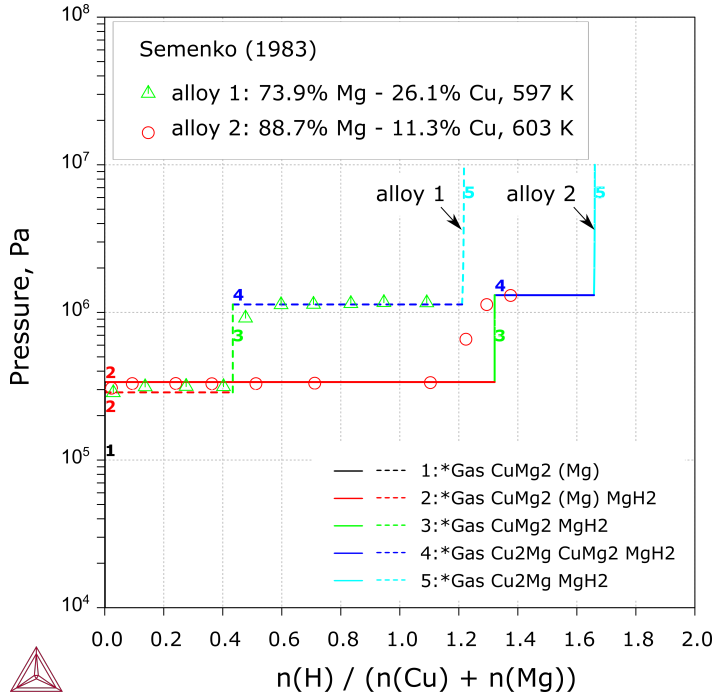

Figure 41: Calculated hydrogen dissolution pressure of two Cu-Mg alloys [2020aChe].

Mg-H-Ni

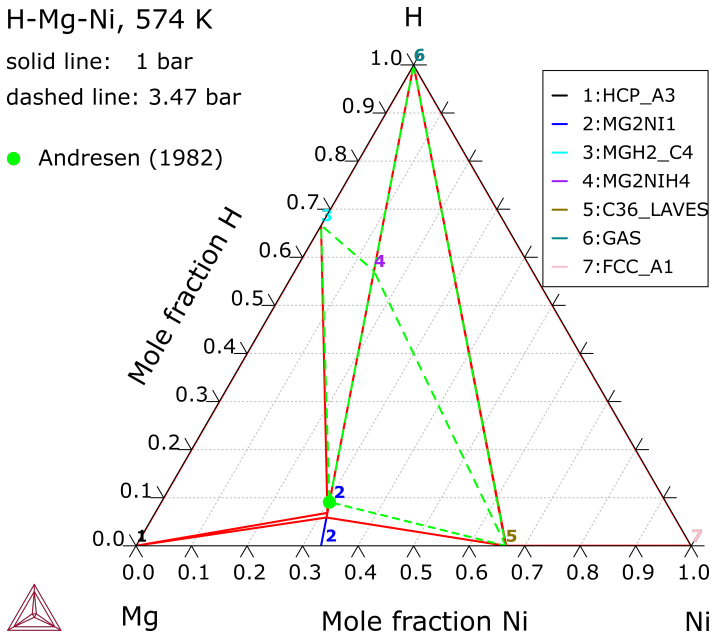

Figure 42: Calculated isothermal section of Mg-H-Ni at 574 K and 3.47 bar [2020Che].

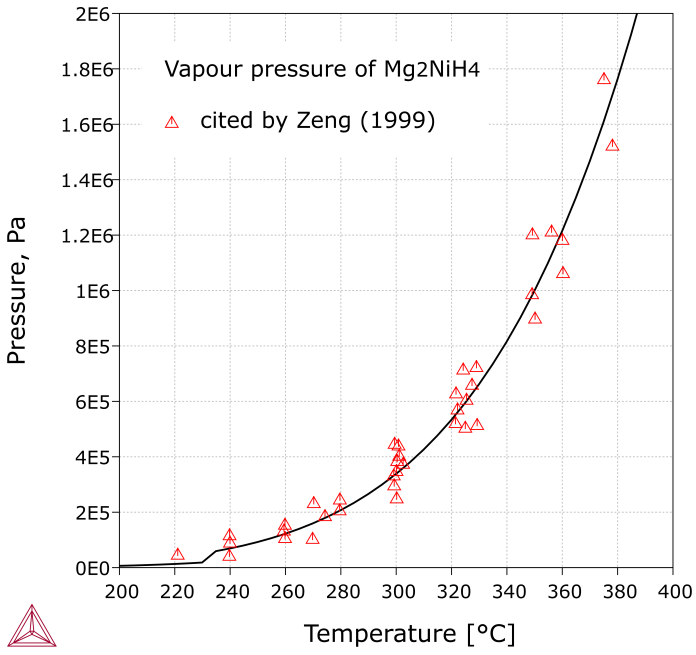

Figure 43: Calculated vapor pressure of Mg_2NiH_4 in the Mg-H-Ni ternary system [2020bChe].

References

[2020aChe] H.L. Chen, Modeling of Cu-H-Mg in TCMG6, Thermo-Calc Software (2020).

[2020bChe] H.L. Chen, Refinement of Mg-H-Ni in TCMG6, Thermo-Calc Software (2020).

Precipitation in Mg-Nd Alloys

The use of the TCS Mg-based Alloys Database (TCMG) with the Add-on Precipitation Module (TC-PRISMA) enables you to do more in depth analysis of such properties as interfacial energy and particle size distribution (PSD).

Important stable and metastable precipitates have been modeled in Mg-RE (rare-earth) alloys. Especially, the bco-type Mg_7RE phase, the $D0_3$-type Mg_3RE phase and the $D0_{19}$-type Mg_3RE phase (RE = Gd, Nd, Y) are modeled.

It is worth noting that whether or not a precipitate is considered metastable depends on the system and the composition. For instance, the MG3R_D03 phase can be a stable phase in the Mg-Nd binary system. When it precipitates in Mg-rich alloys, however, it is considered metastable because eventually it transforms to more stable compounds in this compositional region.

The designations of the precipitates in Mg-RE alloys are not consistent and can be confusing. Taking the Mg-Nd binary as an example, a typical sequence is β'' ($D0_{19}$) > β''' ($Mg_{3-7}Nd$) > β' (Mg_7Nd) >> β_1 ($D0_3$) >> β ($Mg_{12}Nd$) >> βe ($Mg_{41}Nd_5$). β''' ($Mg_{3-7}Nd$) are translation structures between β'' ($D0_{19}$) and β'(Mg_7Nd).

It is beneficial that these stable and metastable phases are modeled in the latest version of the database as this means you can simulate the concurrent nucleation, growth, and coarsening of precipitates during aging treatment in magnesium alloys.

Starting with version TCMG6, and coupled with a compatible atomic mobility database, such as the TCS Mg-alloys Mobility Database (MOBMG) (starting with version MOBMG2), such multi-particle precipitation simulations can be performed with the Add-on Precipitation Module (TC-PRISMA).

In this example, the β_1-Mg_3Nd ($D0_3$) precipitates are simulated as plates [2020d, Chen], where the following settings are entered on the Precipitation Calculator or determined by Thermo-Calc:

- The aspect ratio is fixed at 13.5 according to experimental observation by [2021Hua].
- The interfacial energy is found by Thermo-Calc as 0.029 J/m^2.
- The nucleation site is assumed to be a dislocation considering the extrusion before aging.
- The density is set at the upper limit as 1E16 m^{-2}.
- The mobility enhancement factor is set as 4 .

Read more about the Precipitation Module (TC-PRISMA) on our website. If you are in Thermo-Calc, press F1 to search the help to learn about the available settings included with the Add-on Module.

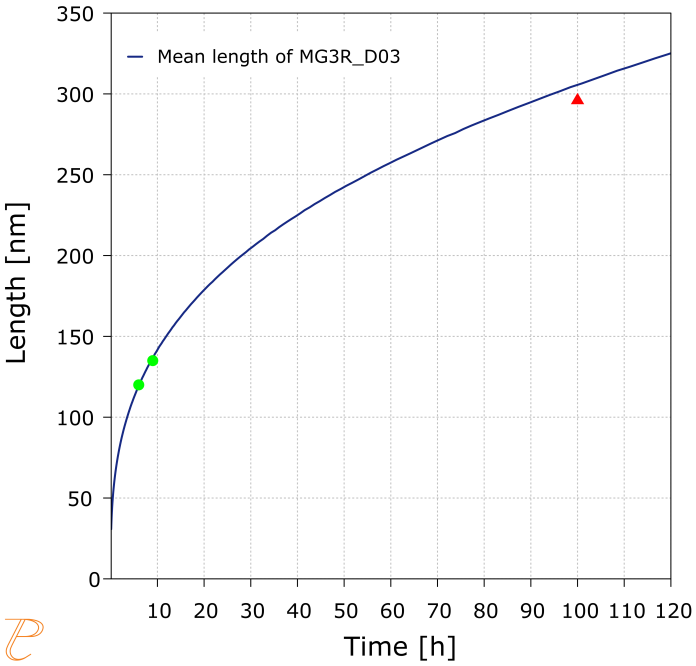

Figure 44: Simulated length of β_1 ($D0_3$) precipitation during aging of an Mg-2.4 wt.% Nd alloy at 523 K for up to 120 h.

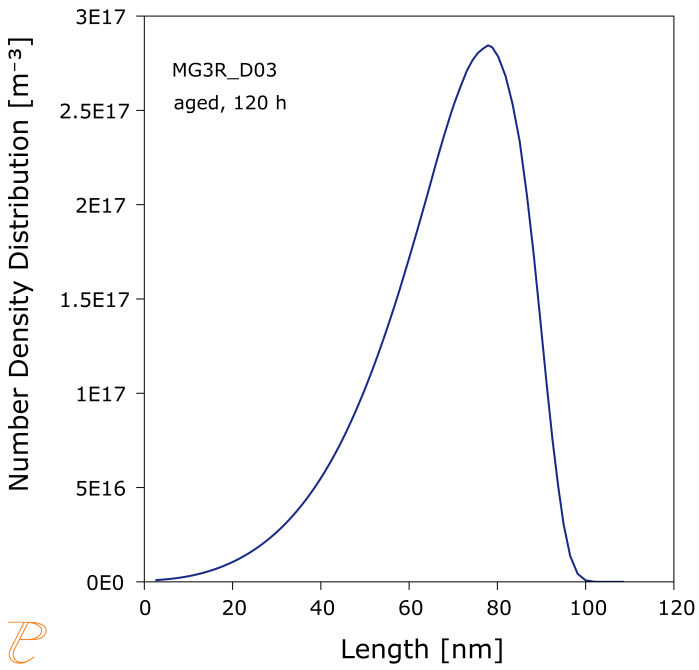

Figure 45: Simulated particle size distribution in the Mg-2.4 wt.% Nd alloy aged at 523 K for 120 h.

References

[2020Che] H.-L. Chen, Modeling Mg-RE (rare earth) metastable precipitates in TCMG6, Thermo-Calc Software (2020).

[2021Hua] Z. Huang, C. Yang, J. E. Allison, L. Qi, A. Misra, Dislocation cross-slip in precipitation hardened Mg–Nd alloys. J. Alloys Compd. 859, 157858 (2021).

Long-period Stacking-ordered (LPSO) Structures

You can use the TCS Mg-based Alloys Database (TCMG) to examine the long-period stacking-ordered (LPSO) structures.

Also see another example about LPSOs: Mg-Y-Zn(-Zr) Alloys.

Liu et al. [2016Liu] experimentally investigated the microstructure of Mg-7Y-4Gd-5Zn-0.4Zr (wt.%) using XRD, DSC, EDS, SEM, and TEM to analyze the microstructure. They annealed the alloy at 300 and 500 °C for 0.5, 5, and 10 h. They found that LPSO-18R precipitates in the Mg matrix in the as-cast state, while with increasing of the annealing time, LPSO-18R transforms to LPSO-14H. It results in substantial improvement of the hardness.

Thermodynamic calculation of the investigated alloy by Liu et al. [2016Liu] using TCS Mg-based Alloys Database (TCMG), versions 7 and higher, can be seen in Figure 46. This shows that LPSO-14H is the stable phase at the equilibrium condition. By suspending LPSO-14H, and redoing the calculation for the same alloy as shown in Figure 47, LPSO-18R appears, which is in good agreement with the results of [2016Liu].

The $Mg_{24}(Y,Gd)_5$ phase that was observed by the experimental work in an as-cast state was not stable in this example calculation. By suspending both the LPSO-14H and LPSO-18R phases, it becomes stable at temperatures lower than 300 °C.

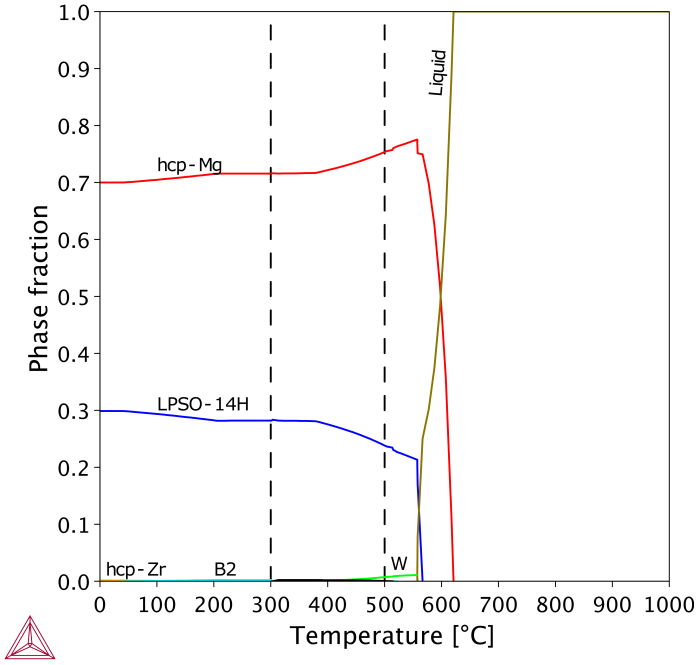

Figure 46: Calculated phase fractions versus temperature for the Mg-7Y-4Gd-5Zn-0.4Zr alloy.

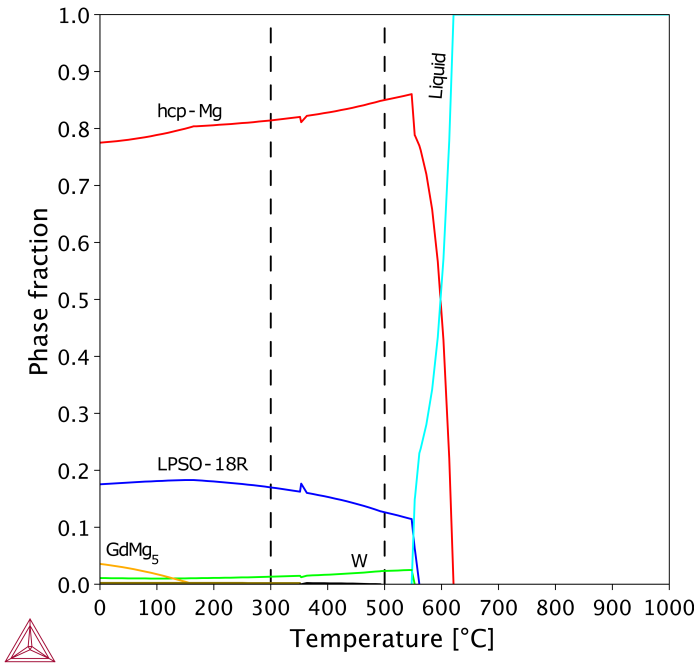

Figure 47: Calculated phase fractions versus temperature for the Mg-7Y-4Gd-5Zn-0.4Zr alloy by suspending the LPSO-14H phase.

Reference

[2016Liu] K. Liu, W. Du, S. Li, Z. Wang, The effect of heat treatment on microstructure of the melt-spun Mg–7Y–4Gd–5Zn–0.4Zr alloy. J. Magnes. Alloy. 4, 99–103 (2016).

Hot Component Application of Mg–Sn–Sr Alloys

Improving high-temperature properties of Mg-based alloys is crucial for hot component applications. Among these, Mg–Sn–Sr alloys show strong potential for enhanced creep resistance. This is primarily due to the beneficial effects of Sn and Sr: Sn contributes to grain refinement, improves corrosion resistance, and forms the thermally stable Mg_2Sn phase. Similarly, Sr also refines grains and forms several stable intermetallic compounds—$Mg_{17}Sr_2$, $Mg_{23}Sr_6$, $Mg_{38}Sr_9$, Mg_2Sr—due to its low solubility in Mg. Furthermore, Sr and Sn can combine to form MgSnSr, another thermally stable intermetallic phase.

RE elements such as Ce, Y, and Gd can further improve mechanical properties. Yang et al. [2014Yan] found that adding 1% Ce, Y, or Gd to Mg–3Sn–2Sr (all wt.%) refined coarse MgSnSr phases, enhancing tensile and creep performance. Moreover, Ce provided the highest tensile strength, and RE-specific intermetallics—$Mg_{12}Ce$, MgSnY, and GdMgSn—were observed.

Fig. 1 shows the phase fraction calculation of the Mg–3Sn–2Sr–1Ce alloy using the latest version of TCS Mg-based Alloys Database (TCMG). The existence of all predicted phases are confirmed by Yang et al. [2014Yan]. Fig. 2 shows the Scheil solidification simulation of the same alloy using the same database. The figure shows that after hcp-Mg solidification, MgSnSr begins to form between 635 °C and 607 °C. In the last stage, remaining liquids transforms to the $Mg_{12}Ce$ intermetallic phase.

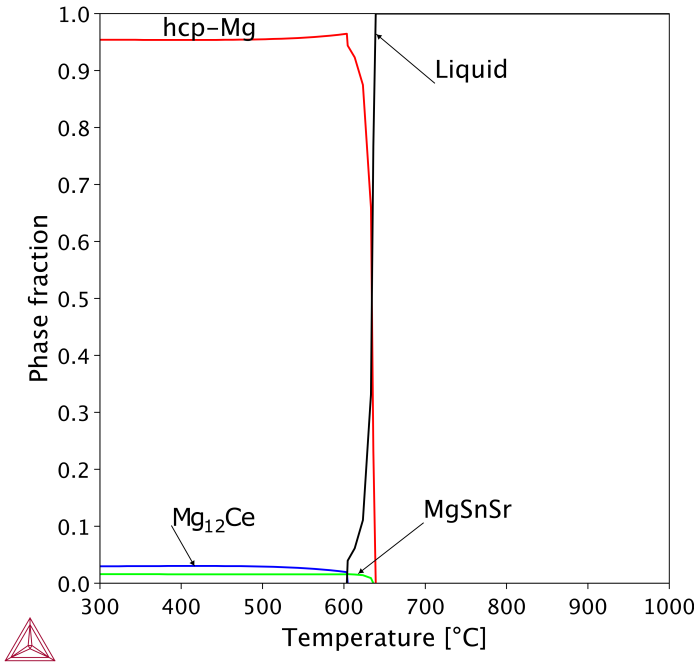

Figure 48: Calculated phase fractions versus temperature of the Mg-3Sn-2Sr-1Ce (wt.%) alloy.

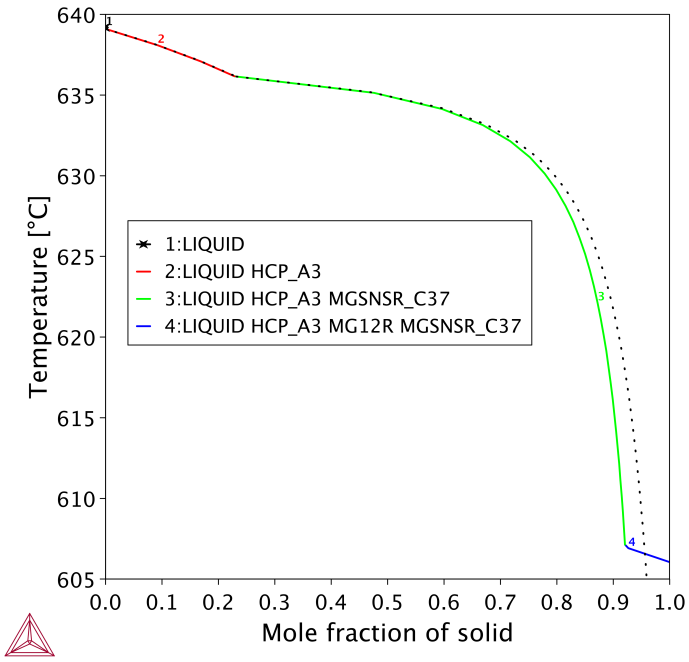

Figure 49: Scheil solidification simulation of the Mg-3Sn-2Sr-1Ce (wt.%) alloy.

Reference

[2014Yan] M. Yang, M. Hou, J. Zhang, F. Pan, Effects of Ce, Y and Gd additions on as-cast microstructure and mechanical properties of Mg-3Sn-2Sr magnesium alloy. Trans. Nonferrous Met. Soc. China 24, 2497–2506 (2014).

Surface Tension: Al-Mg, Al-Zn, and Al-Mg-Zn

The surface tension thermophysical property data is included with the TCS Mg-based Alloys Database (TCMG) starting with version 6 (TCMG6).

For more information about the various thermophysical, thermomechanical, and properties models, and when in Thermo-Calc, press F1 to search the online help. The details are found under a *General Reference* section.

You can find information on our website about the properties that can be calculated with Thermo-Calc and the Add-on Modules. Additional resources are added on a regular basis so keep checking back or subscribe to our newsletter.

Al-Mg

The surface tension of Al-Mg liquid alloys at 973 K is shown. The experimental data are from [1986Gar; 2018Gan].

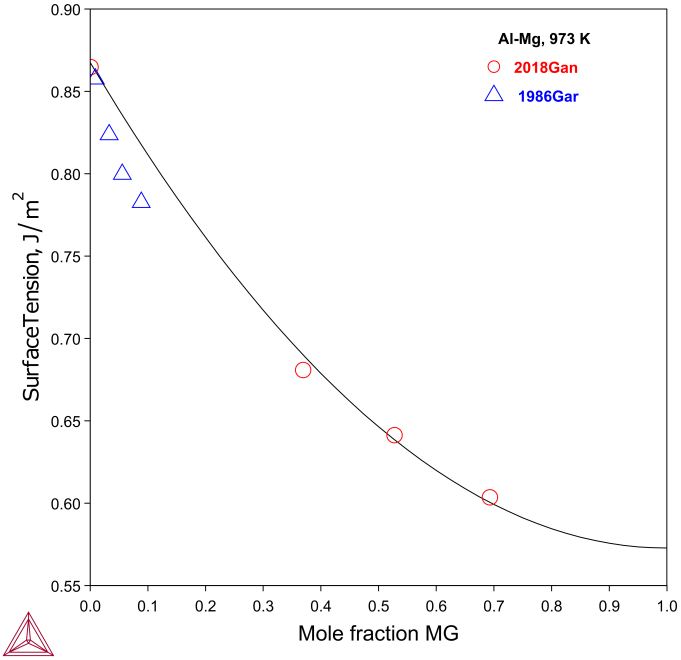

Figure 50: Calculated surface tension of liquid Al-Mg at 973 K along with the experimental data.

Al-Zn

The following plot is the calculated surface tension of Al-Zn binary system along with experimental data from [2016Try].

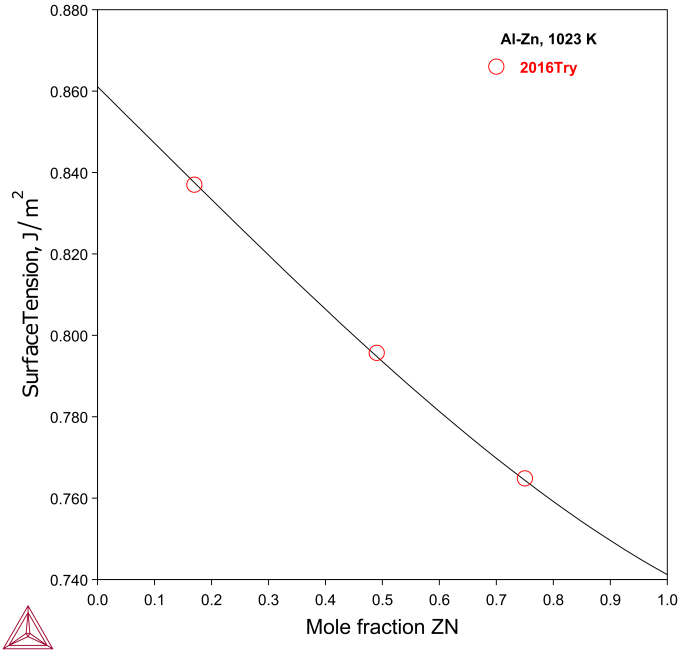

Figure 51: Calculated surface tension of Al-Zn at 1023 K along with experimental data.

Al-Mg-Zn Alloys

The surface tension of Al-67.8-2Zn at%, Al-51.7Mg-2Zn at% and Al-38Mg-1.8Zn at% alloys as a function of temperature is shown.

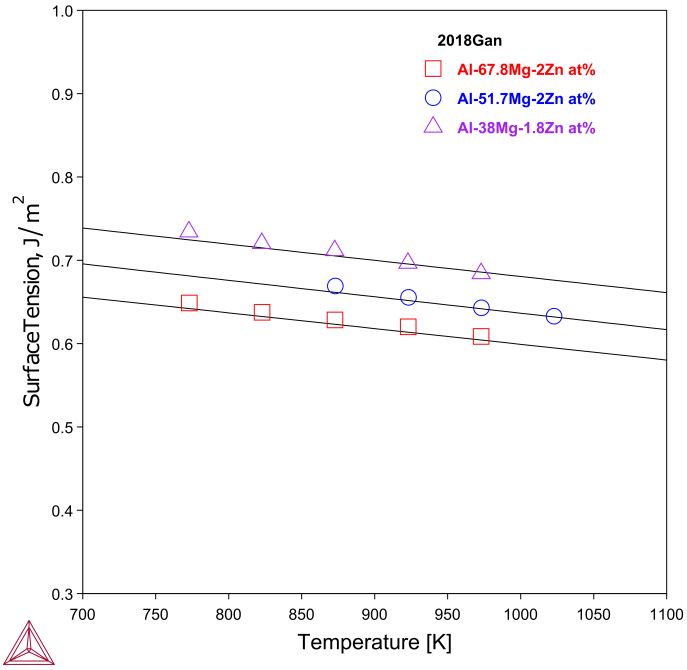

Figure 52: Calculated surface tension of three Al-Mg-Zn alloys as a function of temperature. The experimental data are from [2018Gan].

Reference

[1986Gar] C. Garcia-Cordovilla, E. Louis, A. Pamies, The surface tension of liquid pure aluminium and aluminium-magnesium alloy. J. Mater. Sci. 21, 2787–2792 (1986).

[2016Try] M. E. Trybula, T. Gancarz, W. Gąsior, Density, surface tension and viscosity of liquid binary Al-Zn and ternary Al-Li-Zn alloys. Fluid Phase Equilib. 421, 39–48 (2016).

[2018Gan] T. Gancarz, J. Jourdan, W. Gasior, H. Henein, Physicochemical properties of Al, Al-Mg and Al-Mg-Zn alloys. J. Mol. Liq. 249, 470–476 (2018).

Viscosity: Al-Mg and Al-Mg-Zn

The viscosity thermophysical property data is included with the TCS Mg-based Alloys Database (TCMG) starting with version 6 (TCMG6).

For more information about the various thermophysical, thermomechanical, and properties models, and when in Thermo-Calc, press F1 to search the online help. The details are found under a *General Reference* section.

You can find information on our website about the properties that can be calculated with Thermo-Calc and the Add-on Modules. Additional resources are added on a regular basis so keep checking back or subscribe to our newsletter.

Al-Mg

The viscosity of the Al-Mg system has been extensively studied. There are discrepancies between the measurements of different studies. Based on the higher-order systems, it was decided to use the experimental data from [1959Geb; 2012Li; 2018Gan]. The following diagram shows the dynamic viscosity of the liquid Al-Mg at 973 K.

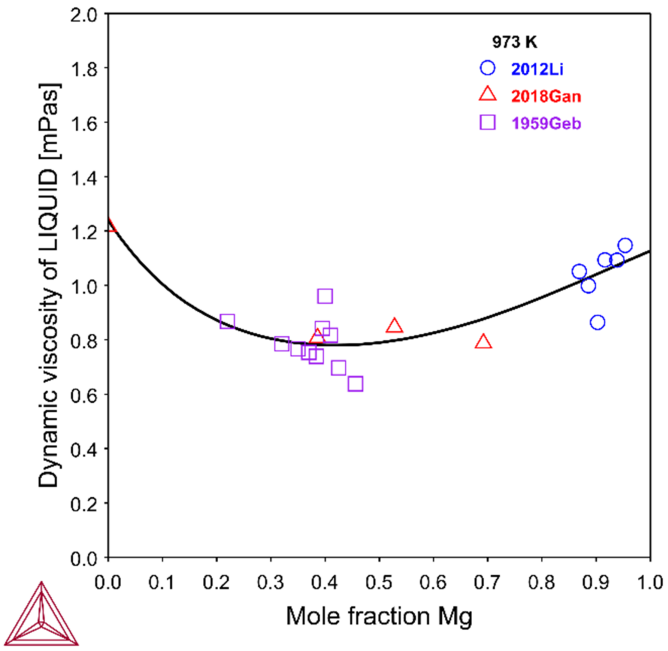

Figure 53: Calculated iso-viscosity plot of the Al-Mg liquid at 973 K.

Al-Mg-Zn

The viscosity of Al-Mg-Zn ternary alloys with charge crucible method was measured in [2018Gan]. Yakymovych [2013Yak] used oscillation cup viscometer for their measurements on viscosity of AL-Mg-Zn alloys. This plot shows the calculated viscosity of two ternary alloys along with the experimental data from these references.

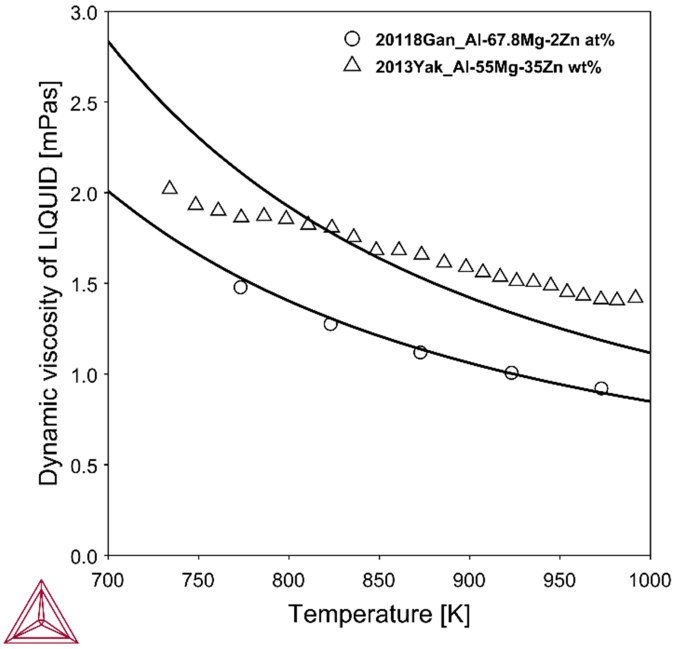

Figure 54: Calculated viscosity of two Al-Mg-Zn liquid alloys.

References

[1959Geb] K. Gebhardt E; Detering, Über die Eigenschaften metallischer Schmelzen: XVI. Die innere Reibung eutektischer Aluminiumlegierungen. Zeitschrift für Met., 379–385 (1959).

[2012Li] P. Li, G. Mi, A. Okhapkin, N. Y. Konstantinova, A. Sabirzianov, P. S. Popel, Micro-mechanism for the evolution of viscosity versus temperature in magnesium-aluminum alloy melts. Procedia Eng. 27, 871–879 (2012).

[2013Yak] A. Yakymovych, Y. Plevachuk, V. Sklyarchuk, “Influence of Zn and Al additions on viscosity of liquid Mg” in Magnesium Technology 2013 (Montreal, Canada, 2013), pp. 1600–1605.

[2018Gan] T. Gancarz, J. Jourdan, W. Gasior, H. Henein, Physicochemical properties of Al, Al-Mg and Al-Mg-Zn alloys. J. Mol. Liq. 249, 470–476 (2018).